5-2017

The Role of the Expansion Segment 7 of 25S rRNA During Oxidative Stress in Saccharomyces cerevisiae

Ethan Gardner
Rowan University

THE ROLE OF THE EXPANSION SEGMENT 7 OF 25S rRNA DURING OXIDATIVE STRESS IN *SACCHAROMYCES CEREVISIAE*

Ethan Gardner B.S.

A dissertation submitted to the Graduate School of Biomedical Sciences, Rowan University in partial fulfillment of the requirements for the M.S. Degree.

Stratford, New Jersey 08084

May 2017

Table of Contents

Table of Contents 2-3

Acknowledgements 4-5

Abstract 6

Introduction 7-23

1.1 The Ribosome 7-9

1.2 Overview of translational machinery 9-12

1.3 Oxidative stress and its effect on translation 12-18

1.3.1. Reactive Oxygen Species: internal and external stressors 13-14

1.3.2. Antioxidant systems 14-15

1.3.3. ROS as signaling molecules that initiate oxidative stress response 15-16

1.3.4. ROS effect on translation: toxic entities vs signaling molecules 17-19

1.4 Research platform for the dissertation: ROS-induced cleavage of 25S rRNA 20-22

1.5 Project objectives 22-23

Rationale 24-25

2.1 To develop and apply ROS-detection protocols to measure oxygen species in cells 24

2.2 To investigate ES7c-cleavage as a possible consequence of apoptosis in yeast 25

2.3 To identify possible intracellular sources causing ES7c-cleavage 25

Materials and Methods 26-30

Experimental Results 31-50

4.1 Characterization of ES7c-cleavage 31-33

4.2 ROS detection development 33-40

4.2.1. Superoxide detection technique 33-37

4.2.2. Hydrogen peroxide detection technique 38-40

4.3 ES7c-cleavage is not a consequence of apoptosis 41-46

4.4 ES7c-cleavage as the result of targeting from an intracellular source 46-50

Discussion 51-56

Summary and Conclusions 57-59

References 60-68

List of Abbreviations 69

Attributes 70

Acknowledgements

First and foremost, I would like to thank my mentor, Dr. Natalia Shcherbik, Ph.D., for allowing me to work in her laboratory. Her skills as a scientist, and her persistent work ethic are truly admirable. Her extensive knowledge of cell biology research was indispensable throughout my time in her laboratory. Not only is she a great scientist, but a wonderful teacher as well. Her support as a mentor kept me going when the project got rough, and she continued providing support until the end. I will be forever grateful to have received her guidance.

I would also like to thank a member of my committee, Dr. Dimitri Pestov, Ph.D., for contributing his resources, time, and knowledge to this project. His expertise certainly contributed to this project. Furthermore. I would like to extend my thanks to the members of Pestov Laboratory, for their assistance and support.

The third member of my committee, Dr. Randy Strich, Ph.D., provided ample contribution and I would like to broadcast my thanks for the expert ideas that he proposed. This project was new to our laboratory (Shcherbik Lab) and his expertise on certain subjects was greatly appreciated.

Thank you to the Rowan University of Biomedical Sciences for providing a degree program that will greatly benefit me on my career path. A special thank you to Dr. Diane Worrad, Ph.D., and Dr. Carl Hock, Ph.D., for their administrative guidance throughout my time in the Master's degree program.

Lastly, I would like to thank my friends and family for their support and encouragement during my time in graduate school. It was the little things that made a big difference.

This project was funded as part of a R01 grant from the National Institute of Health.

Abstract

Translation is an essential process for protein expression in both eukaryotes and prokaryotes. Like any cellular process, translational factors are prone to damage when the cell is under stress. One common stressor that nearly all cells may experience is abnormal levels of reactive oxygen species (ROS). Damage caused by ROS has been associated with disease ranging from neurodegenerative impairments, to the aging process of cells. These oxygen radicals are capable of damaging a litany of molecules including nucleic acids, and molecular factors involved in translation. It has been shown that tRNA can be cleaved upon ROS-induced stress and these fragments come to serve as signaling molecules. However, to date there is very little research that has been done to investigate whether or not rRNAs are capable of similar signaling. Presented in this dissertation is an observed endonucleolytic cleavage in the ES7c region of eukaryotic 25S rRNA, which results in rRNA fragments formation. Herein, experimentation is presented that shows a relationship between elevated levels of ROS, in particular H_2O_2, and ES7c-cleavage. The results presented in this dissertation aim to provide further understanding of this observed rRNA cleavage. The groundwork established during this project serves as a foundation for further research into the nature of this phenomenon. The protocols and procedures that were developed during this project will provide our laboratory with necessary tools for future projects regarding ROS, apoptosis, and rRNA fragmentation.

1. **Introduction**

The main purpose of this Introduction is to briefly describe the structure and function of ribosomes – the major executors of protein synthesis in any living cell. I will also focus on major aspects of translation, highlight the susceptibility of the translational machinery to oxidative stress-related damage, and illuminate oxidative-stress response mechanisms. Additionally, preliminary data and the project objectives, on which my work was built, will also be presented.

1.1 The Ribosome

First discovered in the 1950s by George Emil Palade (Palade, 1955) it was not until much later that the function of the ribosome was understood. In 2009 researchers Venkatraman Ramakrishnan, Thomas A. Steitz and Ada E. Yonath were awarded the Nobel Prize in Chemistry for their work on the crystallized structure of the ribosome (*"2009 Nobel Prize in Chemistry". The Nobel Foundation*). This earlier work eventually illuminated the role of the ribosome as the cornerstone of the translational process and allowed for further structural studies of ribosomal mechanisms.

The ribosome is a hybrid of RNA and protein, termed rRNA and r-proteins. Ribosomes are composed of two subunits, small and large, and in eukaryotes, the small subunit has a constant of sedimentation 40S, while the large subunit sediments with a constant 60S (Ben-Shem et al., 2011). In prokaryotes, the small and large subunits are 30S and 50S, respectively (Pathak et al., 2017). In yeast, ribosomal RNA consists of 25S, 18S, 5.8S, and 5S rRNA (de la Cruz et al., 2015). The reason for the differences in size between the ribosomal subunits of each taxon is the extra sequence of rRNA in eukaryotes. The additional rRNA sequences are referred to as expansion segments (ES). The function of ES is not fully understood, however there is a proposition that ES may serve an additional, regulatory function. In yeast, the largest ES is

known as ES7. This particular segment is a part the 25S rRNA, and is situated on the surface of 60S (Figure 1). It has been shown to be capable of binding multiple proteins, therefore the proposed role for this region is a protein-binding dock (Gómez Ramos et al., 2016).

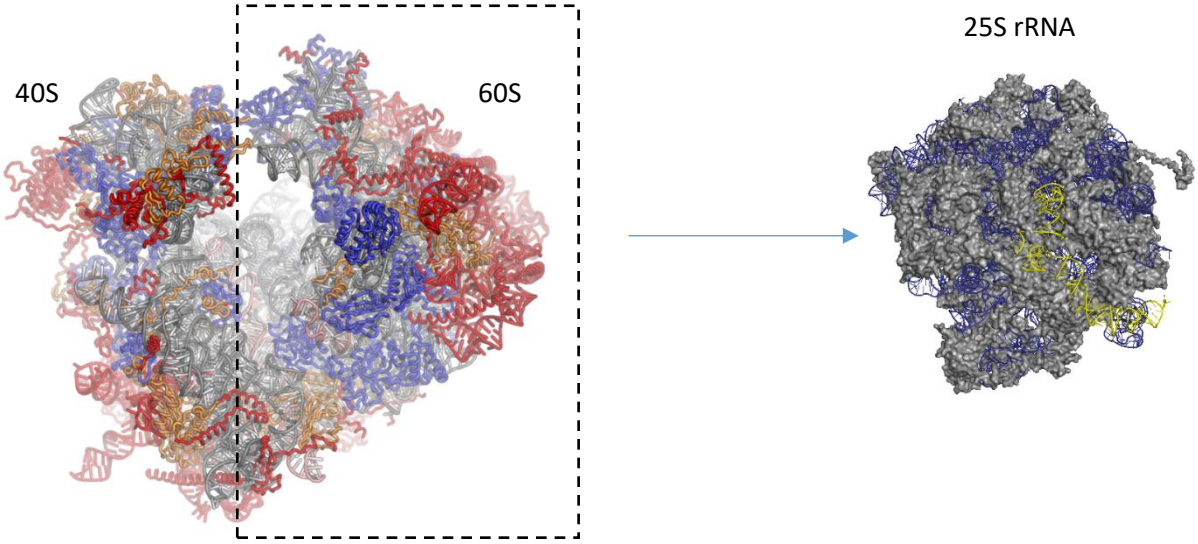

Figure 1: Structure of yeast ribosome. (Left) Assembled 80S ribosomal rRNA composed of 40S and 60S rRNA subunits. The 60S subunit is composed of the 25S rRNA core (right). The 25S structure shows the riboprotein (gray), and the rRNA (blue and yellow). The rRNA sequence in yellow is the ES7c region.

Despite the differences in size between eukaryotic and prokaryotic riosomes, both the large and small subunits function similarly in both taxa. In eukaryotes, the small subunit, composed of both riboproteins and an 18S rRNA core, is generally responsible for mRNA decoding. This subunit ensures that the correct anticodon of incoming tRNA matches with the codon on the mRNA (see Section 1.2). The large subunit, composed of r-proteins and a 28S (25S in yeast) rRNA core in eukaryotes, catalyzes the formation of peptide bonds in the growing chain of amino acids in its peptidyl-transferase center (Steitz, 2008). Each ribosomal subunit is

composed of three active sites: the A site, P site, and the E site. The A site is the initial binding site for aminoacyl-tRNA. It is in this site that the correct aminoacyl-tRNA is base-paired to the mRNA codon in the A site of the small subunit. Upon proper Watson-Crick base-pairing, particular rRNA bases change conformation to accommodate the aminacyl-tRNA. The P site is adjacent to the A site and serves to hold the aminoacyl-tRNA in place while a peptide bond is formed between the A and P site in the large subunit. This secure holding of the tRNA is mediated by interactions with ribosomal protein tails. The deacylated tRNA then moves into the E site where it is eventually released from the ribosome. The major function of ribosomes is to catalyze protein synthesis, the process known as translation. During this process ribosomes cooperate with a large variety of macromolecules, enzymes and factors, to form the translational apparatus. Flawless functioning of translational machinery is required to properly convert genetic information, coded for in mRNA, into a sequence of amino acids ultimately creating proteins.

1.2 Overview of translational machinery

Proteins are a class of molecules, which lie at the heart of nearly all processes within a cell. Proteins can range from small peptides of less than 50 amino acids in length (IUPAC Gold Book, 1995) to large subunit structures that combine to form even larger functional complexes such as RNA Polymerase I, which is nearly 590 kDa in size (Engel et al., 2013).

In order to generate proteins or more complexed multi-subunit protein complexes, peptides must be synthetized first, based on information present in mRNA. This task is accomplished by a process known as translation. Figure 2 provides a basic outline of the translational process in eukaryotes. Translation is a multistep process composed of three stages involving a multitude of various components. For ample details of the translation process, the review by Thomas A. Steitz (Steitz, 2008) is highly recommended. The three stages of protein

synthesis are initiation, elongation, and termination. It is important to note that there are additional steps that occur prior to initiation as well as post-termination that are needed for proper polypeptide synthesis. During this first pre-initiation stage two prerequisites must take place: 1) activation of the carboxyl group of each amino acid, and 2) an established link between the activated amino acids and the proper mRNA coding sequence for the polypeptide. Both of these requirements are addressed by attaching the appropriate amino acid to a tRNA. This attachment employs an ATP-dependent process involving enzymes known as aminoacyl-tRNA synthetases (ARS). The resulting aminoacylated tRNA is now considered charged.

Now that the tRNA is aminoacylated, the next step of the peptide synthesis process is initiation. Initiation requires help from a multitude of initiation factors in the cytosol. First, the coding mRNA binds to the small subunit of the ribosome. In eukaryotes, the initiation factors eIF1A and eIF3 bind to the 40S subunit blocking premature tRNA binding as well as premature assembly of the 60S subunit. Next, another initiation factor called eIF2, binds the charged initiating tRNA as well as GTP. In both bacteria and eukaryotes, this first amino acid is methionine. Now the small subunit of the ribosome scans the mRNA sequence in search of the start codon. With the help of the RNA helicase of eIF4A, as well as other initiation factors, the complex will eventually find the AUG start site. Once the start site has been encountered, initiation factor eIF5B hydrolyzes its bound GTP, which causes the release of the initiation factors. This allows for the 60S subunit to bind and form the fully assembled 80S ribosome. Once fully assembled, the ribosome serves as the binding pocket for incoming aminoacyl-tRNA.

Following the full assembly of the ribosome, the next step in translation is elongation. Similar to initiation, elongation also requires energy in the form of GTP. Moreover, elongation also employs cytosolic factors called elongation factors, which aid the ribosome in polypeptide

chain formation. The first step of elongation involves the binding of a small complex including incoming aminoacyl-tRNA, an elongation factor, and bound GTP to the A site of the 80S initiation complex. Upon binding of the aminoacyl-tRNA, the GTP is hydrolyzed and the elongation factor bound to the now GDP molecule leaves. Next, a peptide bond is formed between the two amino acids in the A site and the P site (where the initiating aminoacyl methionine-tRNA is bound). This bond formation is catalyzed by peptidyl transferase and ultimately deacylates the tRNA in the P site. In the final step of elongation, the ribosome shifts one codon in the 3' direction on the mRNA. This shift moves the newly deacylated-tRNA into the E site where it is released into the cytosol. This movement, known as translocation, requires the elongation factor eEF2 and the subsequent hydrolysis of another GTP molecule. Translocation continues following the steps described above, adding additional amino acids to the nascent polypeptide as the ribosome moves toward the 3' end of the mRNA. Concerning data presented later, it is important to note here that large clusters of ribosomes present on an mRNA transcript are referred to as polysomes. Polysomes can be visualized using sucrose-gradients allowing separation of ribosomal subunits from clusters of ribosomes present on mRNA (Chassé et al., 2017).

Eventually, the ribosome will encounter a stop codon within the mRNA sequence. These codons can be UAA, UAG, or UGA. Once any of these codons enter the A site of the ribosome, release factors hydrolyze the polypeptide linked to the tRNA in the P site, releasing this tRNA (Steitz, 2008). In eukaryotes, the release factor eRF1 recognizes all three stop-codons. With the help of various recycling factors, the release factors also aid the 80S ribosome in dissociating into its 40S and 60S subunits. Additional factors help the dissociating of the mRNA and the tRNA from the small subunit. Upon translation termination, the newly synthesized polypeptide

is released in order to undergo proper folding and processing, resulting in functional protein formation. Due to high abundance of translation machinery factors and executors, numerous stages, and the many complexes that are required for translation, it is easy to see how something could go wrong. Section 1.3 discusses the vulnerability of such an important system in respect to oxidative stress conditions.

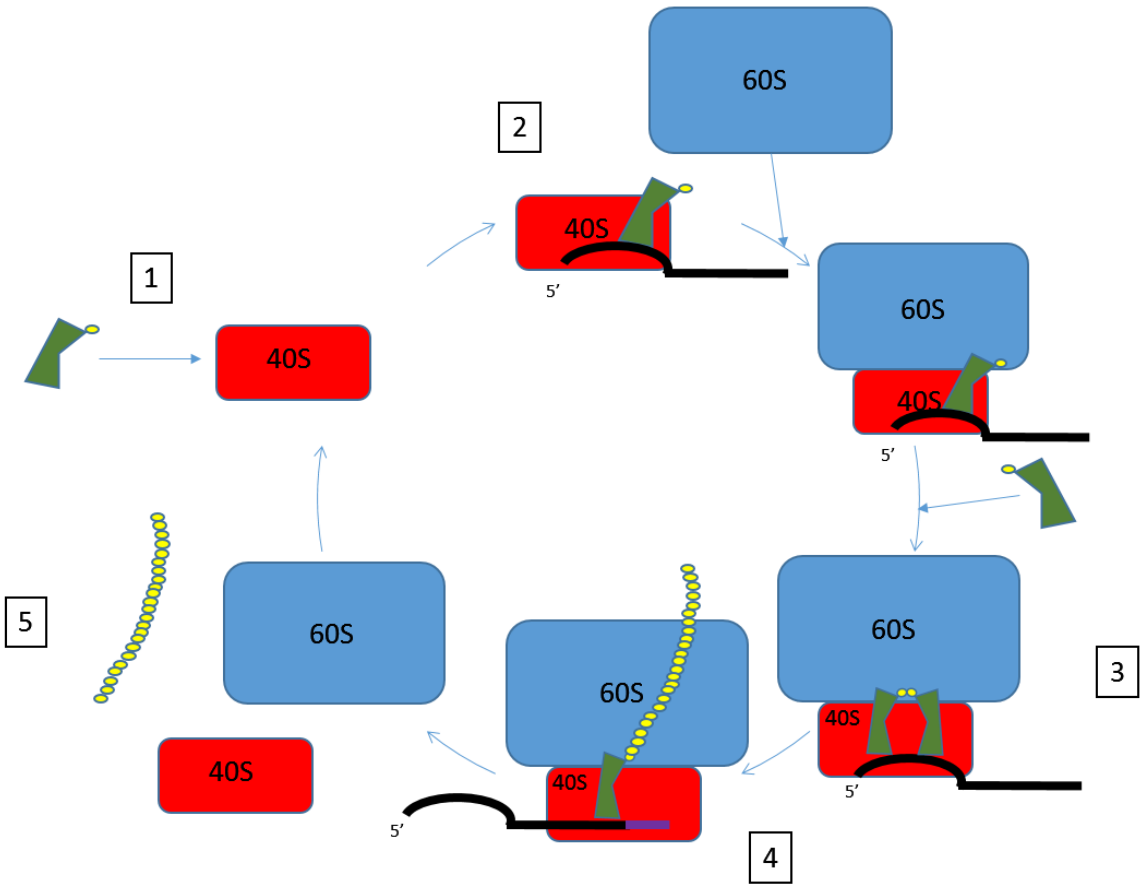

Figure 2: Brief overview of translation in eukaryotes. 1) tRNA is aminoacylated; 2) aminoacylated tRNA and mRNA bind to small ribosomal subunit and large subunit is recruited; 3) successive elongation cycles occur to produce nascent peptide chain; 4) process terminates when stop codon is encountered; 5) ribosomal subunits dissociate and peptide is released for proper folding to occur.

1.3 Oxidative stress and its effect on translation.

During its lifespan, any living cell faces period(s) of unfavorable conditions. Fluctuation of pH, nutrients deprivation, temperature changes, and exposure to toxic substances all cause stress. Unsurprisingly, cells have developed various molecular mechanisms in order to combat and adapt to different kind of stresses. One common stress condition that eukaryotic aerobes encounter is oxidative stress.

1.3.1. Reactive Oxygen Species: internal and external stressors.

Oxidative stress reflects accumulation of reactive oxygen species (ROS), which represent highly reactive chemical species formed upon incomplete reduction of oxygen and include superoxide anions ($\cdot O_2^-$), hydrogen peroxide (H_2O_2) and the hydroxyl radicals ($\cdot OH$). ROS can be supplied externally when cells are exposed to oxidative environments. In aerobic organisms, ROS can be sourced from inside the cell, as byproducts of cellular respiration. Respiration is a process essential to satisfy the energy needs of cells. In eukaryotic aerobes, this process refers to the ATP production via the Electron Transport Chain (ETC). Although this process is required by the cell, it is not without potential problems.

There are numerous sources of ROS that a cell must successfully deal with in order to maintain viability. The ETC in the mitochondria is just one example. Mutations in the ETC pathway, or even dysfunction of the mitochondrial membrane in which the ETC is located, can result in an abnormal concentration of ROS (Eisenberg et al., 2007; Barros et al., 2003). Another possible source of intracellular ROS is the endoplasmic reticulum (Strich, 2015). Dysfunctional protein folding can trigger the production of ROS (Tu and Weissman, 2004). Disruption of the

ER-localized protein folding pathway triggers the upregulation of genes that induce the Unfolded Protein Response (UPR). For example, the yeast *ERO1* is a gene responsible for oxidative protein folding in the ER, which produces H_2O_2 as a byproduct of its mechanism (Zito, 2015). Interestingly, Haynes, et al. (2004) showed that prolonged upregulation of *ERO1* results in an increase in ROS concentration. Furthermore, the UPR-upregulation in the ER as well as the mitochondria contribute to the increase in ROS (Haynes et al., 2004).

1.3.2. Antioxidant systems.

Since stressors such as ROS are such a common encounter, yeast have developed cellular mechanisms to adaptively respond to these stressors (Imlay, 2008). These protective adaptations include both enzymatic and non-enzymatic antioxidant machinery (Jamieson, 1998; Klaunig and Kamendulis, 2004). In an uncompromised eukaryotic cell, enzymes such as superoxide dismutases (i.e. Sod1/Sod2), thioredoxin-dependent peroxiredoxins (i.e. Tsa1, Prx1), and catalases (i.e. Ctt1/Cta1) are capable of reducing these radical oxygen species rendering them harmless (Chae et al., 1994; Wu et al., 2007). Superoxide dismutases, such as Sod1 and Sod2 in yeast provide a means of dealing with superoxide radicals. Sod1 is a cytosolic enzyme, while Sod2 resides in the mitochondrial matrix (Setiey et al., 1975; Cobine et al., 2004). Both enzymes are capable of catalyzing the reaction $2O_2^- + 2H+ \rightarrow O_2 + H_2O_2$ (Bannister et al., 1987).

Other enzymes provide the means of reducing hydrogen peroxide. In yeast, glutathione peroxidase, thioredoxin-dependent peroxiredoxins (Prx) and catalases (CAT) are capable of reducing hydrogen peroxide to water (Chae et al., 1994). Interestingly, these enzymes differ from each other by mechanisms of catalysis. Catalases inactivate hydrogen peroxide in two reactions where one molecule of H_2O_2 oxidizes heme, present in the active center of an enzyme,

generating an intermediate, while a second molecule of H_2O_2 acts as a reducing agent to regenerate the resting state enzyme, producing a molecule of oxygen and water (Switala and Loewen, 2002). This explains why low concentrations of H_2O_2 inactivate CATs; while at high concentrations, CATs break down peroxide. Peroxiredoxins also scavenge H_2O_2 molecules, but do so using a different mechanism. Upon dimerization, oxidation of a catalytic cysteine (Cys) residue of one Prx molecule (resulting in production of sulfenic acid) is followed by the formation of a disulfide bond linkage with a resolving Cys of another Prx molecule. The disulfide bond can then be reduced by thioredoxins (Trx) (reviewed in Rhee and Woo, 2011). Contrary to catalases, Prxs are effective when they are exposed to low levels of free radicals, but lose their peroxiredoxin activity at high concentrations of H_2O_2 by switching to the molecular chaperone function (Jang et al., 2004). This occur due to hyperoxidation of the active-site Cys, resulting in a formation of the sulfinic or sulfonic acids that are susceptible to oligomerization (Lim et al., 2008).

In addition, some of these enzymes are upregulated in response to alternative stressors, including the gene encoding for glutathione peroxidase in yeast (Gpx1) which is upregulated in response to glucose starvation (Ohdate et al., 2010).

1.3.3. ROS as signaling molecules that initiate oxidative stress response.

One striking discovery that has been recently made is that ROS may not always possess a destructive function. At low amounts, ROS, including H_2O_2, function as signaling molecules that activate cellular responses dedicated to prevent buildup of intracellular reactive radicals (discussed in D'Autréaux and Toledano, 2007; Marinho et al., 2014; Winterbourn and Hampton, 2008). The best-studied mechanism of such a signaling function of ROS occurs at the

transcriptional level in both prokaryotes and yeast (Antelmann and Helmann, 2011). It involves thiol-switches that are activated by disulfide bond formation within transcriptional factors. Increasing hydrogen peroxide concentration in the cell would ultimately disrupt the reduced environment of the cytoplasm. Consequently, this net-oxidative environment will lead to the oxidation of thiols and the formation of disulfide bonds (Antelmann and Helmann, 2011). A specific example of this thiol-switch concerns a key regulator of the oxidative stress, the yeast transcription factor Yap1. Transcription factor Yap1 relies on thioredoxin reductases to properly respond to increasing ROS concentrations in the cell (Izawa et al., 1999; Carmel-Harel et al., 2001). More specifically, thiol-cysteine rich sequences located at the C-terminal domain of Yap1 are required for proper localization to the nucleus in response to ROS stress (Kuge et al., 1997). Another example of ROS effects at the transcriptional level is Hsf1 in yeast. This transcription factor is most directly involved in response to acute stresses and upregulates transcription of chaperones and stress proteins (Akerfelt et al., 2010). More importantly, data shows that the Hsf1 transcription factor can respond to increased ROS levels generated from menadione (vitamin K3) as well as thiol oxidants (Yamamoto et al., 2007). Metal centers are another sensing mechanism of ROS. In the gram-positive bacterium *Bacillus subtilis*, it has been shown that transcription factors can even sense ROS concentrations via histidine oxidation catalyzed by iron (Lee and Helmann, 2006). Despite the research showing cells can change their transcriptome in response to stress, the question of whether ROS can signal a stress-response in a process different from transcription remains poorly investigated.

1.3.4. ROS effect on translation: toxic entities vs signaling molecules.

Although yeast cells contain multiple antioxidant systems to combat ROS via their inactivation, problems in these protective pathways (like systems malfunctioning or overloading their functional capacity) may result in an inability to maintain proper (non-harmful) levels of ROS. Left unabated, ROS begin to function as toxic entities capable of damaging essential intracellular components, including DNA, lipids and proteins. These consequences of accumulated ROS might result in detrimental effects on essential cellular processes and therefore contribute to multiple pathologies and aging. One of the targets of toxic activity of ROS is translational machinery.

In Section 1.2, the five major steps of translation are described. Recently published results have shown effects of ROS on transcription at each of the three core steps: initiation, elongation, termination. In 2006, data was published indicating that the transcription initiation factor in yeast, eIF2, is not phosphorylated (not activated) when the cell is exposed to abnormal levels of hydrogen peroxide (Shenton et al., 2006). ROS interference at the elongation phase has also been reported. Work conducted in *Escherichia coli* showed that elongation factor EF-G is inactivated in the presence of increased hydrogen peroxide levels via the formation of disulfide bonds (Nagano et al., 2015). This inactivation of EF-G resulted in retarded synthesis of longer peptides. Lastly, termination may also be affected by ROS levels in the cell (Doronina et al., 2015). It was first shown that elevated oxidation of methionine in the yeast transcription termination factor Sup35 is found in cells under oxidative stress conditions (Doronina et al., 2015). Oxidation of Sup35 converts soluble factors into insoluble [*PSI+*] prion form, which mediates read-through of stop-codons (Sideri et al., 2011, Doronina et al., 2015), ultimately affecting accuracy of translation.

Other examples of detrimental effects ROS can have on translation occur during aminoacylation of tRNA. Efficient protein translation depends on the ratio of correctly acylated to incorrect acylated tRNA. Sulfenylation of Cys182 upon oxidative stress conditions inhibits the editing capacity of the bacterial aminoacyl-tRNA synthetase, ThrRS, and results in protein mistranslation, misfolding and aggregation, manifesting into impaired growth of *E. coli* (Ling and Söll, 2010). Oxidation-dependent mis-acylation of $tRNA^{Gly}$ was also found in *Arabidopsis* and in mammalian cells (Baxter et al., 2007; Netzer et al., 2009). Another example of mistranslation caused by redox stress is oxidation of mRNA, which occurs particularly at guanines. Damaged mRNA promotes ribosome stalling (Simms et al., 2014) and generation of aberrant polypeptides susceptible to aggregation (Tanaka et al., 2007). This manifests itself in a range of neurodegenerative diseases, including Lewi-bodies dementia, Alzheimer's, and Parkinson's diseases (Nunomura et al., 2002; Nunomura et al., 1999; Zhang et al., 1999).

ROS targets are not always translational factors composed of proteins. It has been shown that under oxidative stress conditions mature tRNAs undergo nucleolytic cleavages, resulting in a diverse set of tRNA-derived fragment formation (reviewed in Raina and Ibba, 2014). Interestingly, these fragments, termed tRFs, turned out to not be molecular artifacts, but regulatory molecules. It was found that tRFs are capable of targeting ribosomes and thus, contribute in regulating translation during oxidative stress (Gebetsberger et al., 2012; Anderson and Ivanov, 2014).

Ribosomes, the major executors of the translation process, are also targets of ROS. However, information describing effects of ROS on structure/function of ribosomes is extremely limited. To the best of my knowledge, the only study publicly available investigated effects of severe oxidative stress on rRNAs in yeast (Mroczek S, Kufel J., 2008). It was found that

exposure of yeast cultures to stimuli known to induce apoptosis, such as high concentrations of H_2O_2, acetic acid, hyperosmotic stress, and ageing, results in fragmentation and subsequent degradation of rRNAs from both ribosomal subunits. Consequently, when intracellular ROS levels rise to amounts that are incompatible with life the cell turns on the apoptotic program, rRNAs undergo a sequence of nucleolytic cleavages followed by rRNA-fragment degradation in order to dispose of the overabundant nucleic acid. However, questions on how low-level and/or temporary oxidative stress may affect rRNAs, the backbone of a ribosome, or whether rRNAs may function as a source of signaling molecules (in analogy with tRNA's, tRFs) remain unexplored. In fact, being the most abundant RNA in the cell, rRNA may be capable of influential roles similar to that of tRNA. Further exploring the possibility of rRNA fragments serving as signaling molecules in response stressors, such as ROS, may reveal additional roles for rRNA to play at the translational level.

1.4 Research platform for the dissertation: ROS-induced cleavage of 25S rRNA.

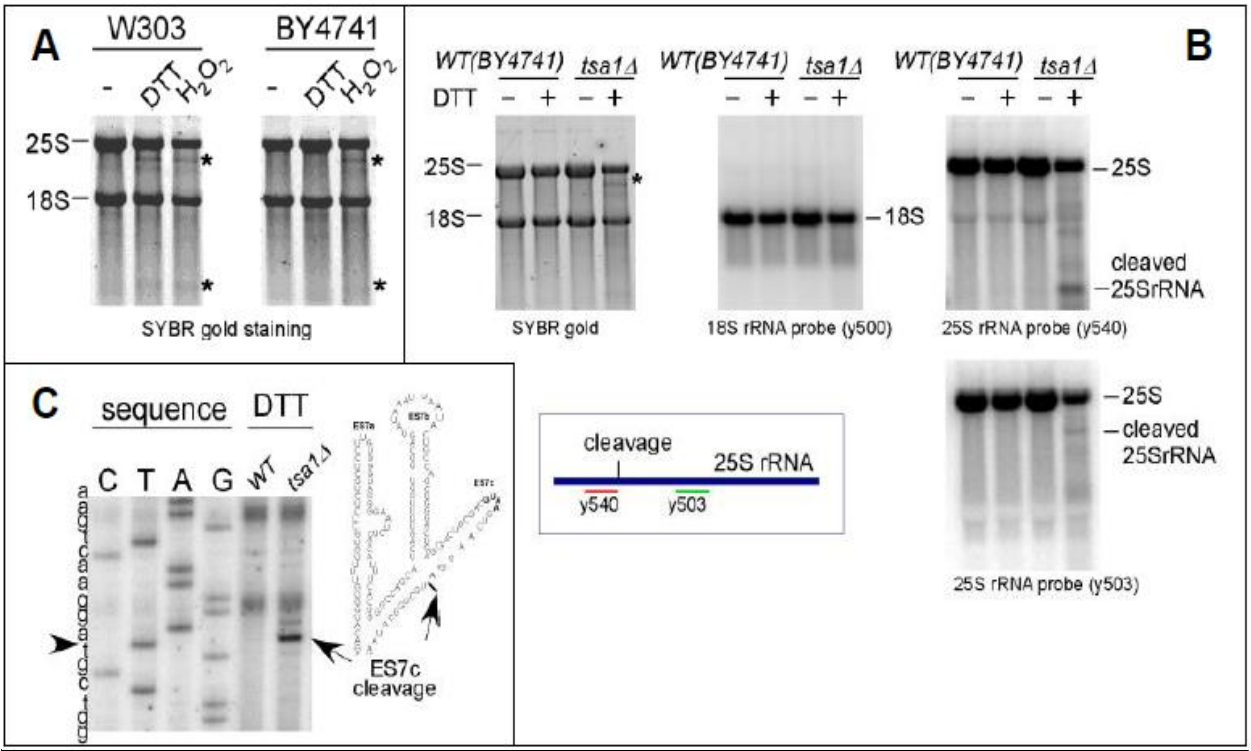

Figure 3. 25S rRNA undergoes endonucleolytic cleavage in the ES7c region upon DTT treatment. (A) Cells from W303 and BY4741 strains were grown in YPDA to mid log phase at 30°C, treated with 20mM DTT for 2 hrs or remained untreated. Total RNA was analyzed by SYBR gold staining. Asterisk indicates position of RNA fragments (3kB and 0.6kB). (B) Cultures from *tsa1* and its isogenic WT control (BY4741) strains were treated with DTT as in (A). Total RNA was analyzed by SYBR gold staining and by northern hybridization with radioactively labeled probes against 25S and 18S rRNAs. Annealing positions of y503 and y540 on 25S rRNA are shown in the inset. (C) Primer extension analysis (right) for the cleavage site in the 25S rRNA in *WT and tsa1* cells treated with DTT. Sequencing of a plasmid containing 25S rDNA (left) was performed with the same primer as used for the primer extension analysis. The secondary structure and cleavage site of ES7c are shown. (Courtesy of N. Shcherbik)

As stated in Section 1.1, yeasts' ribosomal RNA consists of 25S, 18S, 5.8S, and 5S rRNA (de la Cruz et al., 2015). Of these rRNAs, the 25S is most important to this dissertation; more specifically, the expansion segment 7 (ES7). Expansion segments are unique to eukaryotic ribosomes with ES7 being the largest within the 60S subunit. Moreover it is suspected that these segments may retain a regulatory role (Gómez Ramos et al., 2016). Although such a regulatory role for ES7 has been predicted, the exact mechanisms of its functioning remain elusive.

The preliminary work conducted in the laboratory has shown that treatment of yeast cells with the reducing agent dithiothreitol (DTT) induces cleavage of the 25S rRNA in the ES7c region (Figure 3C). We showed that the same cleavage was detected upon treatment of yeast cultures with ROS inducers including an inorganic H_2O_2, menadione, and plumbagin (Figure 3A & Figure 5). Northern hybridizations combined with primer extension technique mapped this cleavage to be located at the ES7c region of 25S rRNA (Figure 3B&C, Figure 4). A mutant for

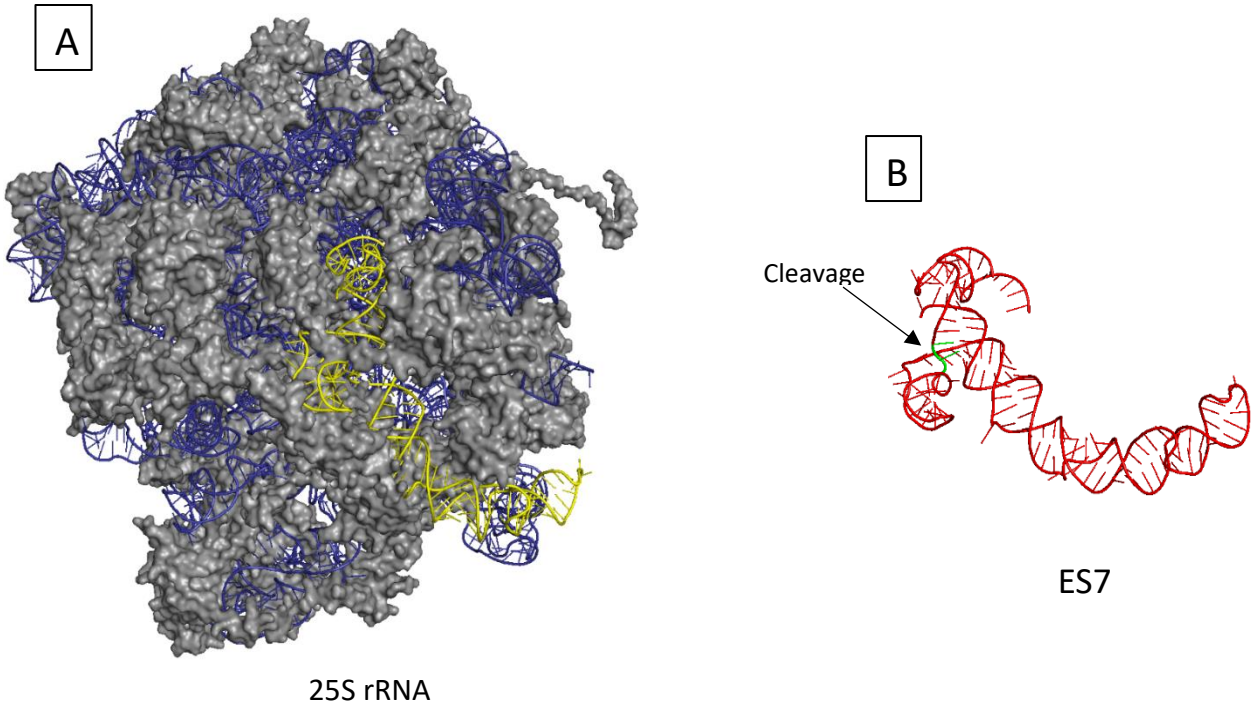

Figure 4: Structural model of 25S subunit and ES7 region. A) 25S subunit of yeast. Riboprotein highlighted in gray; rRNA highlighted in blue and yellow; ES7 region highlighted in yellow. B) Isolated ES7 region. Cleavage site (ES7c) mapped via primer extension is highlighted in green.

the *TSA1* gene was used in the mapping experiments as it displayed high sensitivity towards DTT. In fact, *TSA1*, which encodes the peroxiredoxin Tsa1 in yeast, has been identified in genetic screens as a gene that provides resistance to harmful effects of DTT (Rand and Grant, 2006). After endonucleolytic cleavage was mapped to the ES7c region of the 25S rRNA, we

used PyMOL software to create 25S rRNA structure with the ES7 region highlighted in yellow (Figure 4A). Figure 4B shows the isolated ES7 region with the mapped site of cleavage shown in green. ES7, like nearly all expansion segments, is specific for eukaryotic ribosomes, located on the surface of 60S and functions as a regulatory region of the ribosome (Gómez Ramos et al., 2016).

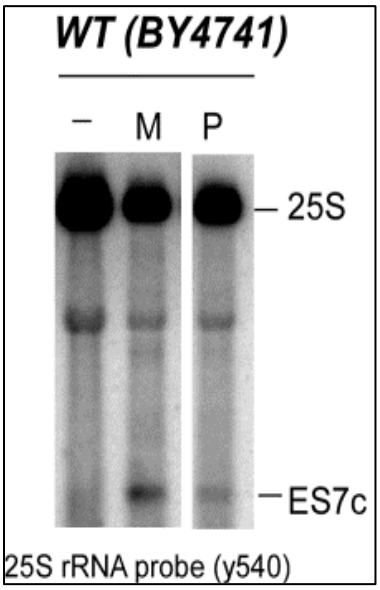

Figure 5. ES7c cleavage induced by various oxidative agents. *WT* cells were untreated (-), treated with 100uM menadione (M), or 12.5uM plumbagine (P) for 4 hours. Total RNA was extracted, resolved on agarose gel under denatured conditions and transferred on nylon membrane. Northern hybridization was performed with radioactively labeled probe against 25S rRNA y540. (Courtesy of Dan Shedlovski).

One possible explanation for the unexpected effect of DTT on 25S rRNA integrity is that DTT does not act as a reducing agent to induce rRNA fragmentation, but rather promotes ROS formation. In support of this hypothesis, several studies have found that oxidation of DTT results in production of oxygen radicals, *in vitro* (Biaglow and Kachur, 1997; Held et al., 1996). Thus, we propose that ES7c-cleavage is a consequential cellular response to the elevated levels of ROS.

1.5. Project objectives

As stated in Section 1.3.4, ROS might have a dual function in a cell. At high levels, ROS, in particular H_2O_2, function as toxic entities damaging various cellular components, including RNA and RNA-containing complexes like ribosomes. However, at low amounts they can initiate oxidative stress-response and target not only protein factors, but RNA molecules too, as was shown for tRNA fragments. We have detected formation of 25S rRNA-derived fragments in

response to ROS. However, we did not know whether this fragmentation is a product of ribosome degradation due to oxidative stress-induced apoptosis, or if the 25S rRNA cleavage in ES7c region (hereafter, ES7c-cleavage) functions as oxidative-stress signaling event. Therefore, two hypothesis emerged: 1) the ES7c-cleavage might be an early marker of yeast apoptosis, which hasn't been described before; 2) or that ES7c-cleavage functions as cellular response to an oxidative stress, when stress is not harsh enough to induce apoptosis. If this hypothesis is correct, we envision the possibility that cleavage of 25S rRNA in the ES7c region might constitute an early marker of oxidative stress, and possibly plays a role in oxidative stress signaling. The "oxidative stress-response/signaling" model, proposed here to explain the nature of 25S rRNA fragmentation, **constitutes the central hypothesis of this study**.

The major goal of my dissertation work was to develop experimental approaches, which would allow us to distinguish between "the early-apoptosis marker" and "the stress-response" models of ES7c-cleavage of 25S rRNA.

2. **Rationale**

The means by which oxidative stress affects eukaryotic ribosomes is not well understood. The single current study reported extensive cleavage of rRNAs in response to severe oxidative conditions, and this effect of ROS on rRNA integrity was attributed to being a part of an apoptotic program (Mroczek and Kufel, 2008). This dissertation attempts to expand the limited knowledge of alterations yeast ribosomes may experience when cells are subjected to various levels of oxidation, including low-dose oxidative stress.

The preliminary data generated in the laboratory prior to my Masters of Science work has demonstrated that treatment of yeast cells with the reducing agent DTT causes a single endonucleolytic cleavage of 25S rRNA in the "c" loop of the expansion segment 7 (ES7c) (Figure 3C). Similar effect was observed upon treatment with oxidants, like inorganic H_2O_2 (Figure 3A), menadione and plumbagin (Figure 5). Based on these data, and the knowledge that DTT might cause ROS production in cells (Xiang et al., 2016), the laboratory proposed that ES7c-fragments production might be a result of oxidative stress. My goals within this project are formulated as follows:

2.1 To develop and apply ROS-detection protocols to measure oxygen species in cells.

To address the "ROS-induced ES7c-fragmentation" hypothesis experimentally, I evaluated amounts of ROS generated in cells subjected to the ES7c-cleavage-inducing treatments. I focused on establishing the methodology for reliable detection and measurement of superoxide and hydrogen peroxide in yeast cell. Besides looking at ROS accumulation upon drug treatment, these new-to-laboratory assays allowed examination into whether ES7c cleavage is a response to a specific radical, or if it represents a universal response to elevated levels of ROS.

2.2 To investigate ES7c-cleavage as a possible consequence of apoptosis in yeast.

Here, using a combination of biochemical, genetic and molecular techniques, I investigated whether ES7c-cleavage might be a part of an apoptotic program. One of the protocols I was involved in establishing in the laboratory was the Annexin V staining. Staining of cells with Annexin V represents a commonly-accepted approach of early apoptosis detection. In addition, I tried to established an alternative way of early-apoptosis detection, which is based on release of Cyc1 (cytochrome C) from mitochondria, as this event lays upstream of translocation of Annexin V's substrate (phosphatidylserine, PS) to the surface of the cell.

2.3 To identify possible intracellular sources causing ES7c-cleavage

The final goal of my work was focused on determining a source of the ES7c cleavage. Upon preliminary experimentation, drug treatments (external to a cell stress stimuli) were assumed to have been the source of the observed ES7c-cleavage. Consequently, it was deemed prudent to investigate whether this cleavage can occur from intracellular signals. More specifically, the question on whether this cleavage occurs via ROS sourced from the ER, mitochondria, was addressed.

3. Materials and Methods

Cell strains: All strains are listed in Table 1.

Yeast media, drugs, and treatment conditions: Standard PCR-based techniques were used to generate deletions (Longtine et al., 1998). YPDA media was used as standard (1% yeast extract, 2% peptone, 2% dextrose, 10mg/L adenine). Synthetic control (SC) media was also used when needed. Yeast cultures were grown overnight. The following day the cultures were diluted into fresh YPDA media to OD_{600} =0.2 and grown for an additional 2-3 hours at 30°C. Various concentrations, indicated in the figure legends, of drugs were used to treat cells. Drugs included DTT (Sigma Aldrich, Cat. No. D9779), H_2O_2 (Sigma Aldrich), menadione (Enzo Life Sciences, Cat. No. ALX-460-007-G010), or plumbagin (Acros Organics, Cat. No. EW-88197-37). Scavenging hydrogen peroxide employed the use of 10μM ebselen (TCI, Cat. No. 60940-34-3). Cell cultures grown in YPDA were exposed to ebselen for 1 hour prior to treatment with redox drugs.

ER-stress was induced using 1μg/mL tunicamycin (Calbiochem, Cat. No. 11089-65-9) for 2 hours. Mitochondrial stress was induced using 20μg/mL rotenone (Kaya et al., 2015) available from Tocris (Cat. No. 83-79-4).

RNA extraction and Northern blotting: Total RNA was extracted from cell samples using a single-step extraction method using formamide-EDTA. Extracted RNA was separated on 1.2%agarose gel containing 1.3% formaldehyde (Mansour and Pestov, 2013). RNA was transferred to H-Bond nylon membrane (GE Biosciences, Cat. No. RPN119B). Visualized

probed rRNA using methylene blue or SYBR-gold (Thermo Fisher, Cat. No. S11494). Northern hybridization was performed using ^{32}P-labeled oligonucleotide probes (Pestov et al., 2008).

Probes: y500 against 18S rRNA (5'-AGAATTTCACCTCTGACAATTG), y503 against 3'-end of the 25S rRNA (5'-ACCCACGTCCAACTGCTGT), and y540 against 5'-end of the 25S rRNA (5'-TCCTACCTGATTTGAGGTCAAAC).

Spliced (*HAC1*^{i}) and non-spliced *(HAC1*^{u}*) HAC1* were visualized by hybridizing membranes in Church buffer (6326095). Probe is for *HAC1* exon and recognizes both *HAC1*^{i} and *HAC1*^{u} (Back et al., 2005). Probe was generated via PCR using genomic DNA template and primers Forward primer: 5'-AGCGGATCCATGGAAATGACTGATTTTGAAC and the Reverse primer: 5'-TCTTGATCACTGTAGTTTCCTGGTCATC. All hybridizations were imaged using a Typhoon 9200 Phosphoimager and accompanying ImageQuant software (GE Biosciences).

Primer extension: Primer extension analysis used total RNA extracted from *WT* and *tsa1Δ* cells treated with 20mM DTT for 2 hours at 30°C. A total of 3µg of RNA was separated on the guanidine-containing gel and RNA fragment of interest (i.e. 3kB ES7c-fragment) was extracted as described in (Wang et al., 2015). The extracted RNA was annealed with 2pmol of [^{32}P]-labeled primer (Prex1: 5'- GACTCCTTGGTCCGTGTTTC) by incubating the mixture at 65ºC for 5 minutes, and primer extension reaction was performed as described in (Kent et al., 2009). For reverse transcription we used MonsterScript RT (Epicenter). Reaction products were purified by phenol/chloroform extraction, precipitated with ethanol,

dissolved in 10μL of loading buffer (95% formamide, 10 mM EDTA, 0.1% xylene cyanol, and 0.1% bromophenol blue, at final pH 11) and analyzed on a 6% polyacrylamide/urea gel. The sequencing reaction was performed with SequiTherm EXCEL II (Epicentre) using 250ng of rRNA expression plasmid pJD694 (Rakauskaite and Dinman, 2008) as a template and [^{32}P]-labeled Prex1 primer. Sequencing reactions were resolved next to primer extension reaction products. Gel was dried, exposed onto a phosphorimager screen (GE Biosciences) and developed using a Typhoon 9200 PhosphorImager and ImageQuant software (GE Biosciences).

ROS detection: Cells from overnight culture were grown to mid-log phase and treated with DTT (as described above). $4x10^6$ cells were analyzed using Amplex Red. Cells were then collected and washed in PBS and suspended in 0.5mL of the supplied Reaction Buffer. Incubation was performed for 30 minutes at 30°C, and collected by centrifugation. Samples were stained with either Amplex Red or dihydroethidium as follows:

dihydroethidium (ThermoFisher, Cat. No. D23107): 5mM dihydroethidium (stock 5μg/mL) was added to samples. Samples were incubated for 30 minutes in the absence of light before they were ready for sampling.

Amplex Red Reagent (ThermoFisher, Cat. No. A12222): Horseradish peroxidase was added to catalyze Amplex Red reaction. Hydrogen peroxide levels were determined by inserting samples into a 96-well plate and recording the fluorescent signal at 590nm using a Biotek Synergy H1 microplate reader. Hydrogen peroxide signal calibration curve was created using the linear range of H_2O_2 fluorescence. P-value was determined by paired, two tail t-test.

Apoptosis: Overnight culture of wild-type cells (*BY4741*) was back diluted with YPDA to OD_{600}≈0.2, grown for additional 4 hours at 30ºC, and treated with oxidative drugs for various periods of time as indicated in figure legends. Cells were collected by centrifugation, washed, and converted to spheroplasts using techniques developed/modified in our laboratory in combination with a protocol published in (Lee et al., 2017). Spheroplasting was performed using Zymolase T-100 (Sunrise science products) at the final concentration of 30 μg/mL in spheroplasting buffer (0.8 M D-sorbitol, 10 mM β-mercaptoethanol, 20 mM Tris-HCl, pH 7.4) for 15 minutes at 30°C. Efficiency of spheroplasting was determined microscopically. Spheroplasts were washed twice with PBS (pH 7.0), once in 1X binding buffer supplied with the ApoDETECT Annexin V-FITC kit (ThermoFisher, Cat. No. 331200) containing 0.6M D-sorbitol. Spheroplasts (2×10^6 cells) were treated with FITC-Annexin V and propidium iodide (Sigma-Aldrich, Cat. No. P4864) according to the manufacturer's recommendation. Annexin V-FITC stained spheroplasts were analyzed using a BD Accuri C6 flow cytometer (Model 23-13244-04) and FlowJo® software (version 10).

Cytochrome c-GFP cloning (adapted from Roucou et al., 2000): Cytochrome c was cloned into a 2μc, tryptophan-selectable plasmid containing GFP at the N-terminus under a TEF promoter (obtained from Dimitri Pestov). Cytochrome c-GFP was then cut out and fused with plasmid pESC-HIS (GenTech) in order to use histidine as the selectable marker. mtRED (obtained from Katrina Cooper) was expressed in transformed cells, which contains mitochondrial localization sequence attached to RFP.

Cell viability and growth: Culture of *BY4741* strain was started at a volume of 5 mL (OD_{600}≈0.2) and was grown at 30°C shaking for 4 hours (OD_{600}≈0.8 after 4 hours). Afterwards, culture was divided into 4 mL aliquots and treated with 25 µM, 50 µM, or 100 µM menadione, or 5µM, 16µM, 25µM rotenone. Samples were placed into 96-well plates in triplicate. The plates were incubated at 30°C for 24 hours in a microplate reader (Biotek) recording OD_{600} at set intervals.

Table 1. Yeast strains

Strain	Genotype	Reference
BY4741	*MAT***a** *his3-1 leu2-0 met15-0 ura3-0*	Open Biosystems
tsa1Δ	*MAT***a** *his3-1 leu2-0 met15-0 ura3-0 tsa1Δ::KANMX6*	Open Biosystems
ire1Δ	*MAT***a** *his3-1 leu2-0 met15-0 ura3-0 ire1Δ::KANMX6*	Open Biosystems
tsa1Δ ire1Δ	*MAT***a** *his3-1 leu2-0 met15-0 ura3-0 ire1Δ::KANMX6 TSA1::LEU*	This study
aif1Δ	*MAT***a** *his3-1 leu2-0 met15-0 ura3-0 aif1Δ::KANMX6*	Open Biosystems
yca1Δ	*MAT***a** *his3-1 leu2-0 met15-0 ura3-0 yca1Δ::KANMX6*	Open Biosystems

4. Experimental Results

Prior to presenting data that addressed my goals stated in the Objectives and the Rationale of this dissertation, I would like to describe other results that I generated, while my project was in its initial state. The results presented below reflect our attempt to characterize ES7c-fragments of 25S rRNA using various approaches.

4.1 Characterization of ES7c-cleavage.

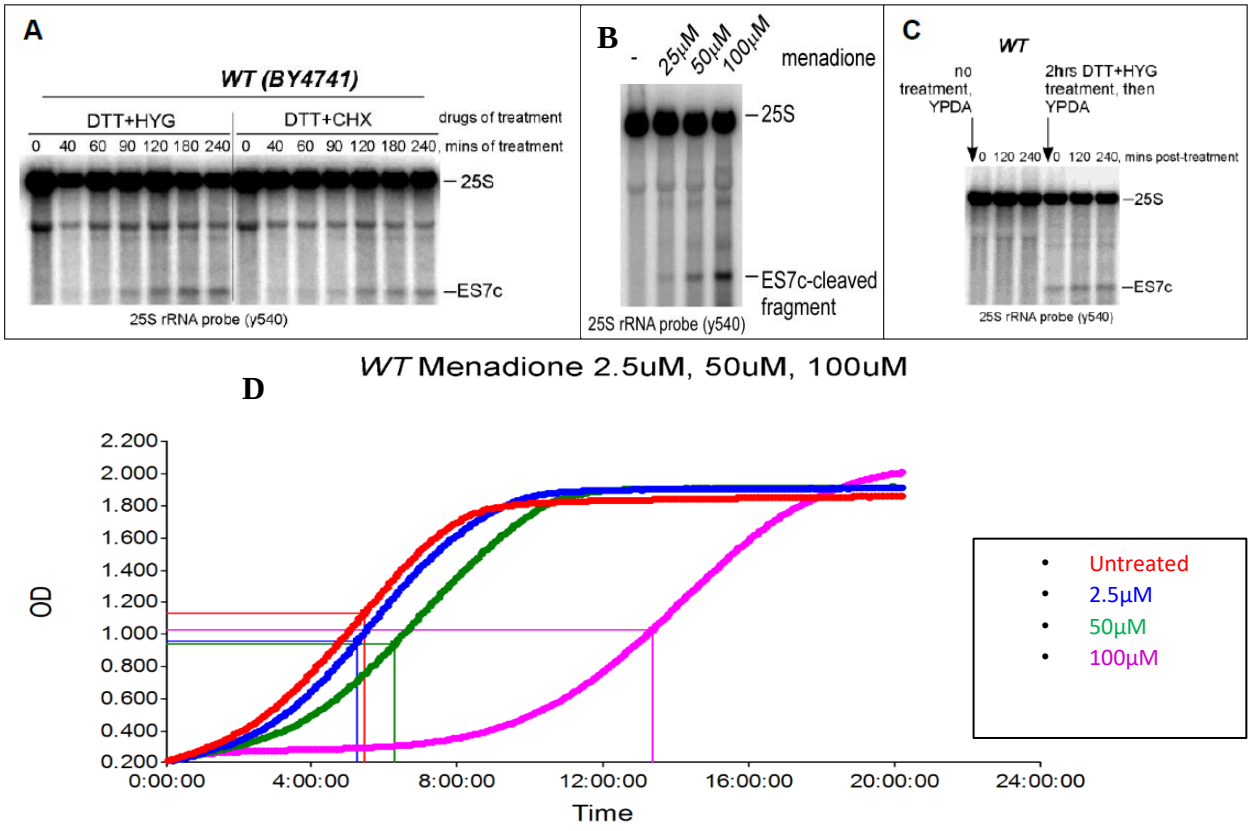

Figure 6. ES7c cleavage occurs quickly post-drug treatment and results in formation of stable rRNA fragments. (A) Cells from BY4741 were treated with DTT and 500ug/mL of HYG (left) or DTT and 100ug/mL of CHX (right). Cells were collected at the indicated time points, and RNA was extracted and analyzed as described in Methods.. (B) Analysis of ES7c-cleavage formation upon treatment of BY4741 cells with titration of menadione concentration (courtesy of Daniel Shedlovsky); (C) Cells from BY4741 were grown in YPDA media to mid log phase at 30°C, treated for 2 hours with DTT+HYG to induce stalling or remained untreated. Cells were washed to remove drugs and suspended in YPDA. Chase was performed for indicated periods of time. Total RNA was extracted from cells and analyzed by Northern hybridization using y540 probe against 25S rRNA. D) Growth curve of wild-type cells treated with indicated doses of menadione over a 24 hour period.

The initial study of the ES7c-cleavage formation in response to DTT treatment was conducted in *tsa1Δ* cells. We wondered why *tsa1Δ* cells are more susceptible to DTT-induced cleavage within the ES7c region compared to wild-type cells (Figure 3B). One of the working hypotheses was that lack of functional peroxiredoxin (Tsa1) might cause ribosome stalling. To test this hypothesis, we induced stalling of ribosome in wild-type cells using two translational inhibitors: cycloheximide (CHX) and aminoglycoside hygromycin B (HYG). We found that drug-induced stalling indeed increased sensitivity of yeast ribosomes towards rRNA-cleaving effects of DTT in time-dependent matter (Figure 6A). A similar effect of ES7c-cleavage formation was detected upon titration of menadione (Figure 6B), which is another oxidant found to induce ES7c-cleavage (Figure 5). Finally, a post-treatment experiment demonstrated that the ES7c-fragments formed upon DTT treatment are stable over time (Figure 6C). A remaining possibility was that this cleavage product was nothing more than an artifact of extremely sick/dying cells. To address "the health of cells" upon oxidant treatment we monitored growth of wild-type cells in liquid cultures, treated with menadione (Figure 6D). To stay consistent with previous data, in this assay, we used the same concentrations of menadione (25μM, 50μM and 100μM) as for Northern blot analysis, demonstrated in Figure 6B. Although growth of cells was significantly inhibited at 100μM menadione, cells treated with 25μM, and 50μM menadione grew similarly to non-treated control. Although the latter concentrations of the drug did not affect cell growth, the ES7c-fragments were readily evident (Figure 6B). Taken together, these data indicate that endonucleolytic cleavage within 25S rRNA represents a fast response to oxidative stress conditions resulting in formation of stable fragments.

In addition, the sucrose density sedimentation analysis of ribosomal species extracted from *tsa1Δ* cells treated with DTT revealed that cleaved ribosomes are present in polysomal

fractions (data not shown). The data suggest that the ribosomes undergoing ES7c-cleavage were in fact translating ribosomes or those that were engaged in translation.

4.2 ROS detection development

4.2.1. Superoxide detection technique.

The main assay for detection of superoxide radicals involved the use of dihydroethidium. In its reduced state, this compound emits a blue fluorescence signal in the cytosol. However, upon oxidation by superoxide dihydroethidium is converted to ethidium, which intercalates with nucleic acids. Additionally, the oxidation of dihydroethidium shifts the fluorescence emission signal from 518nm to the red spectrum at 635nm.

To detect superoxide presence in cells by dihydroethidium, cells from BY4741 yeast strains were grown overnight in YPD media. The following day, cells from overnight culture were back-diluted to an OD600 of 0.3, and grown for another 2-3 hours to allow for logarithmic growth. Induction of superoxide radicals was accomplished by exposing cells to 100µM menadione or 1mM H_2O_2 (Suzuki et al., 2017). Untreated wild-type cells were used as a negative control to confirm that the redox drugs were in fact raising the level of ROS in the treated cells. Menadione-treated *sod1Δ* and *sod2*Δ cells served as a positive control (refer to Section 1.3.2). Consequently, *sod1Δ/sod2Δ* mutants lack the ability to convert superoxide to hydrogen peroxide, thereby affirming that superoxide radicals will accumulate. Sod1 is a superoxide dismutase that resides in the cytoplasm, while Sod2 is localized in the mitochondria. Cells were incubated with dihydroethidium for 30 minutes. The treated samples were immobilized on glass slides and observed under a fluorescent microscope at 63x objective power.

Figure 7 shows the results of treatment with dihydroethidium. A mutant for the peroxiredoxin Tsa1, was included as a reference since earlier work showed that mutants for this peroxidase are susceptible to redox stress (Trotter and Grant, 2002). Moreover, *tsa1Δ* showed high efficiency of ES7-cleavage (Figure 3B-C). In wild-type untreated cells, there is a significantly lower amount of detectable signal fluorescing from the cells when compared to the oxidative-stress inducing treatments (Figure 7A & B). As predicted with the *tsa1Δ* there is a higher amount of signal across both untreated and drug-treated samples. When originally experimenting with this particular protocol, 100µM menadione was used initially. After just 1 hour, cells showed signs of stress and ES7c-cleavage was observable (discussed later). However, hydrogen peroxide treatment takes 2 hours to show signs of stress in cells. For this reason, treatment of menadione was decreased to 50µM, but treatment time was increased to 2 hours to coincide with H_2O_2 treatment. The latter condition (50µM menadione, 2 hours long treatment) corresponded to the experimental set up used for Northern blotting (Figure 6B) and growth assay (Figure 6D) analyses.

Figure 8A shows the same assay except using *sod1Δ* and *sod2Δ* cells. These mutants lack the ability to reduce superoxides, ultimately resulting in a buildup of superoxides in the cells. Drug treatment conditions are the exact same as those used in Figure 7. When compared to wild-type in the previous experiment, it is clear to see that the fluorescent emission observed in *sod1Δ* and *sod2Δ* is more intense across all samples, both treated and untreated (Figure 8A). This is to be expected and indicates that dihydroethidium is capable of detecting superoxide radicals under our experimental treatment conditions.

Now that superoxide levels could be monitored, we treated the same *sod1Δ* strain with both menadione and H_2O_2 to evaluate ES7c-cleavage (Figure 8B & C). The strain *yap1Δ* is null for

the gene encoding for the transcription factor Yap1. This transcription factor is a key regulator of oxidative stress response (Okazaki et al., 2007) and was used as a positive control.

In both treatment conditions, *sod1Δ* cells showed comparable to wild-type cells levels of cleaved fragment in both treatment conditions (Figure 8B & C). As predicted, superoxide levels were shown to be much higher in *sod1Δ* cells upon drug-treatment (Figure 8A), however there were no significant increases in ES7c-cleavage in these cells, concluding that superoxide does not affect ES7c-cleavage.

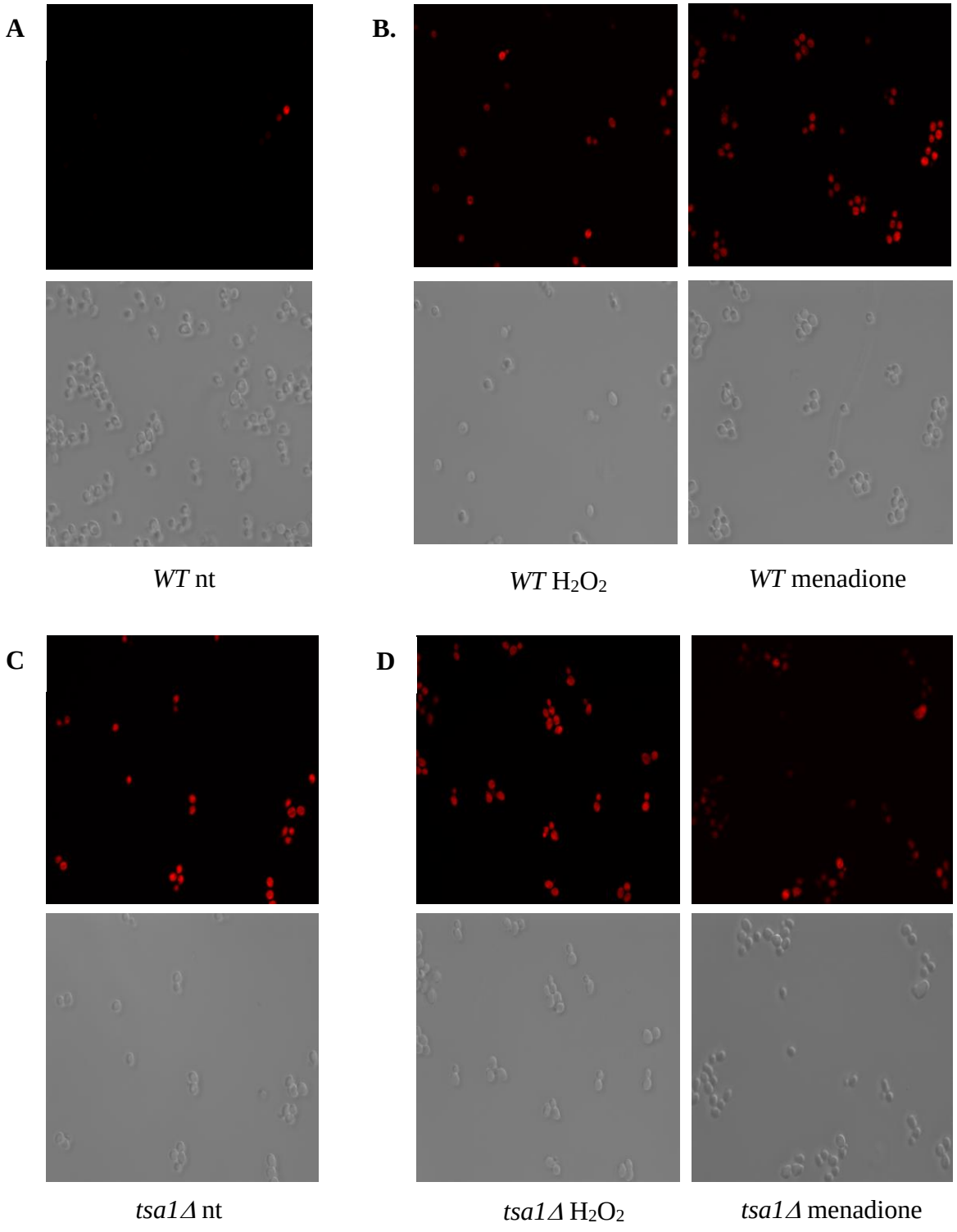

Figure 7. ROS detection using dihydroethidium staining. In all panels, top image is the red fluorescence channel, while the bottom image is the Nomarski image of same field of view. A) *WT* cell without any drug treatment (denoted "nt"). B) *WT* cells treated with 1mM H_2O_2 or 50μM menadione. C) *tsa1Δ* cells without treatment. D) *tsa1Δ* treated with 1mM H_2O_2 or 100μM menadione.

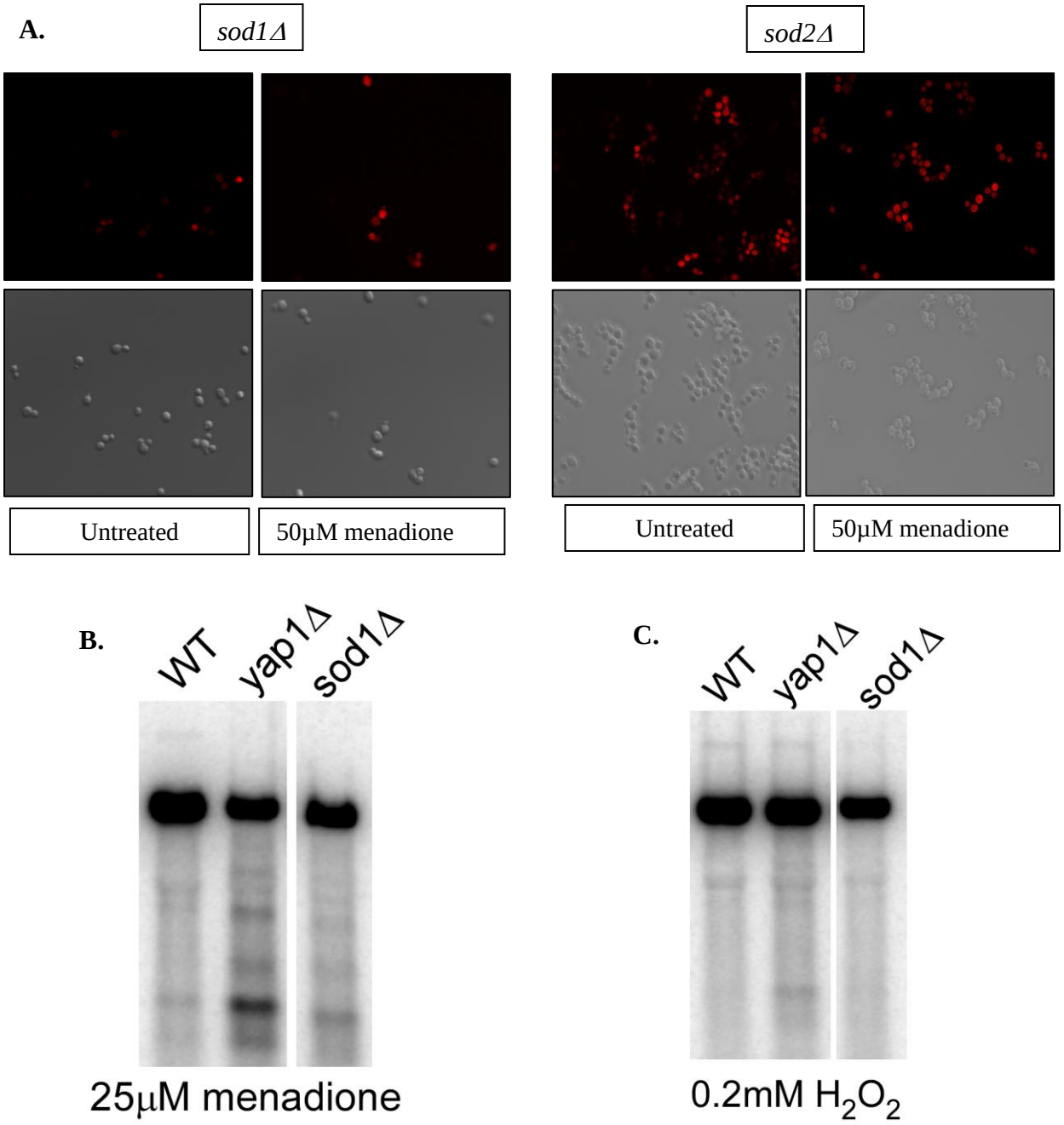

Figure 8. Superoxide detection in *sod1Δ* and *sod2Δ* cells. A) Dihydroethidium assay to detect superoxide ROS levels. This figure includes the *sod1Δ* and *sod2Δ* mutant strains, which serve as positive controls for induction of superoxide ROS. For each mutant strain an untreated control sample and a sample treated with menadione were incubated with 5μg/mL of dihydroethidium and observed under a fluorescent microscope. B & C) Northern hybridization of mutants treated with menadione or H_2O_2 to induce cleavage (*yap1Δ* serves as positive control). Probe used is y540.

4.2.2. Hydrogen peroxide detection technique.

There are multiple different types of ROS existing in the intracellular environment (see Introduction). The second form of abundant ROS species that we were eager to measure was hydrogen peroxide. The main assay for this detection experiment involved the reagent Amplex Red, which reacts quickly with H_2O_2 in the presence of horseradish peroxidase (HRP) to produce resorufin (Wang et al., 2017). In order to determine the concentration of H_2O_2 in the cells treated with DTT, fluorescent signals from Amplex Red were compared to a calibration curve built using known concentrations of inorganic H_2O_2. The experiment was performed three times in order to ensure replicability. Comparing DTT-treated cells to untreated cells, a standard T-test indicated significance at $p<0.05$. These results indicate that we have recorded proper conditions in which hydrogen peroxide concentration can be measured. Cells treated with DTT showed a significantly elevated level of H_2O_2 in both 2 hour and 4 hour treatment when compared to the respective untreated samples (Figure 9A).

Next, we wanted to observe the ES7c-cleavage phenomenon under the same treatment conditions so as to compare the hydrogen peroxide levels to ES7c-fragmentation. *WT* cells were grown into logarithmic growth and then treated with ROS-inducing drugs. Northern hybridization reveals strong cleavage from all drug treatments (Figure 9B). Furthermore, this shows that in concordance with elevated hydrogen peroxide levels, there is also an elevated level of ES7c-cleavage product. This suggests that the ES7c-cleavage may occur from hydrogen peroxide, however this conclusion required one last experiment.

Ebselen is capable of scavenging for H_2O_2 significantly lower hydrogen peroxide levels in the cell (Satheeshkumar and Mugesh, 2011). 10µM ebselen was added to *tsa1Δ* cells for one hour, while another aliquot of the same culture did not receive the scavenger treatment. Both

cultures were then treated with 20mM DTT for 0, 15, and 30 minutes. RNA extracted from these cultures was analyzed by Northern hybridization. Compared to the control (ebselen-free) sample, cells that received pre-treatment with ebselen exhibited observably lower levels of ES7c-cleavage (Figure 9C). In conclusion, it would appear that ES7c-cleavage occurs in response to hydrogen peroxide either directly or indirectly.

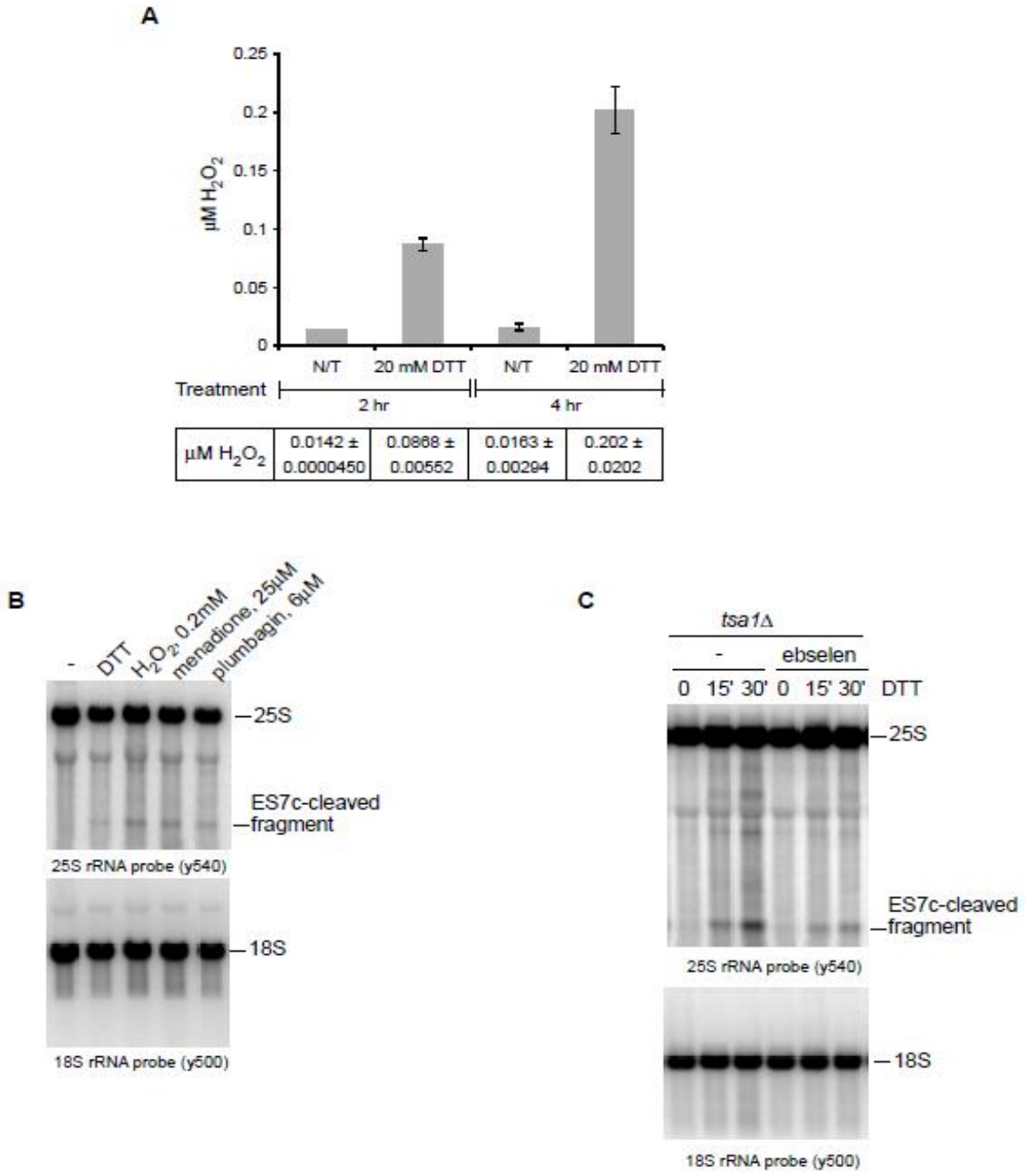

Figure 9. Hydrogen peroxide detection. A) Cells were grown to mid-log phase in YPDA media. Cells were treated with 20mM DTT for 2 hours or 4 hours at 30°C. Cells were then harvested and washed with PBS. Amplex Red assay was performed according to protocol. (Figure courtesy of Daniel Shedlovskiy). B) Northern hybridization for ES7c fragment. Cells were treated with ROS –inducing drugs for 2 hours except for H_2O_2 treatment which lasted 30 minutes. C) *tsa1Δ* cells were grown to logarithmic phase and treated with ROS-scavenger, 10μM ebselen, or not treated with the scavenger. Then samples were treated with 20mM DTT and hybridized with 25S probes (y540), and 18S probe (y503). (Figure courtesy of Natalia Shcherbik).

4.3 ES7c-cleavage is not a consequence of apoptosis.

A study conducted in laboratory of Joanna Kufel has addressed the fate of yeast ribosomes during severe oxidative stress that ultimately caused apoptosis (Mroczek and Kufel, 2008). Thus, it was found that upon treatment of yeast wild-type cells with various oxidants, 25S rRNA undergoes extensive fragmentation resulting in production of multiple rRNA fragments, including those that are formed by ES7c-cleavage (Mroczek and Kufel, 2008). Although our work has detected ES7c-cleavage formation in cells subjected to mild oxidative stress, the question of whether or not this cleavage is a part of apoptotic program remained unanswered.

Apoptosis is a unique form of cell death. It is a genetic process that has been observed under a variety of cellular stress conditions ranging from ROS, to aging (reviewed in: Strich, 2015). Knowledge about apoptosis led to procurement of the possibility that the ES7c-cleavage fragment is a product of programmed cell death.

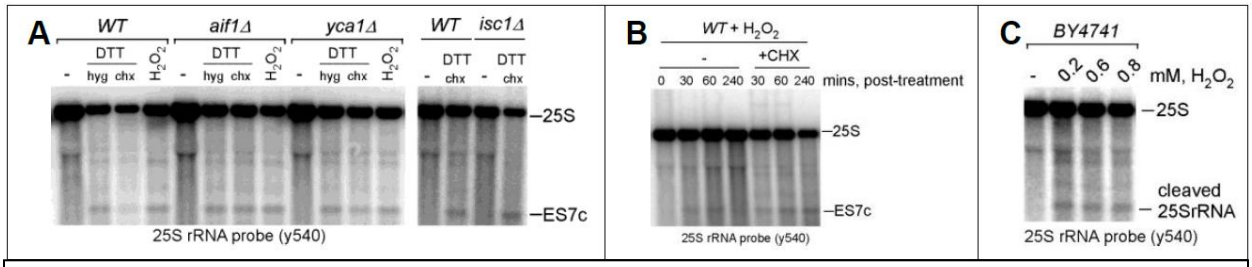

Figure 10. Inhibition of apoptosis does not affect ES7c-cleavage of 25S rRNA. (A) Cells from indicated yeast strains (all on BY4741 background) were grown in YPDA media to mid log phase at 30°C, treated for 2 hours with DTT+HYG or DTT+CHX or for 30 mins with 0.2mM H2O2 to induce ES7c cleavage. Total RNA was extracted from cells and analyzed by Northern hybridization using y540 probe against 25S rRNA. (B) Cells from BY4741 strain were treated for indicated periods of time with 0.8mM H2O2 in the presence (+CHX) or absence (-) of CHX. CHX was used in this experiment to inhibit apoptosis. Total RNA was prepared and analyzed as in (A). (C) Cells from BY4741 strain were treated with 0.2mM, 0.6mM and 0.8mM of H2O2 for 30 mins or remained untreated. Total RNA was prepared and analyzed as in (A).

To address this, we used three yeast strains containing deletions for apoptosis-inducing genes (*yca1Δ*, *aif1Δ* and *isc1Δ*), treated them with DTT, and assessed ES7c-cleavage formation (Figure 10A). We reasoned that if ES7c-cleavage of 25S rRNA is part of apoptotic program, its

formation must be suppressed in apoptosis-defective cells. We detected formation of the ES7c-fragment in tested apoptosis-defective strains (Figure 10A). Besides genetic intervention (Figure 10A), we inactivated apoptosis via the translational inhibitor, cyclohexamide (CHX), and examined ES7c-fragment formation. Since CHX has been found to prevent apoptotic cell death induced by hydrogen peroxide (Madeo et al., 1999), we treated cells with 1mM H_2O_2 for various periods of time, including a 240 minute treatment which has been shown to be an apoptosis-inducing condition (Mroczek and Kufel, 2008). H_2O_2 treatment was done in two parallel cultures with and without CHX supplementation. As expected, treatment of cells with H_2O_2 for 240 minutes resulted in excessive fragmentation of 25S rRNA visible as a smear on the Northern blot (Figure 10B, lane 4), suggesting that the apoptotic cell death program is active under this condition. Inhibition of apoptosis with CHX eliminated 25S rRNA-derived smear at 240 minutes, but did not affect formation of the ES7c-fragment (Figure 10B, lanes 5-7). Finally, the ES7c-cleavage was also observed in wild-type cells during short treatment time with very low doses of inorganic H_2O_2, further suggesting that apoptosis may not be involved (Figure 10C).

Together, this data suggests that the observed ES7c-cleavage is unlikely to be a part of an apoptotic pathway. Nonetheless, both Yca1 and Aif1 are involved in mid to late apoptosis (Madeo et al., 2002; Wissing et al., 2004), creating a possibility that the ES7c-cleavage might still be a part of an apoptotic program, occurring during initial, early stage of apoptosis. If this turned out to be the case, cleavage of 25S rRNA in the ES7c region would represent an “early marker of apoptosis”. To investigate this possibility, we exploited an early hallmark of apoptosis, deterioration of the mitochondrial membrane (Green and Kroemer, 2004), to find a connection (if any) between level of rRNA cleavage and induced apoptosis.

To further address the possibility that ES7c-cleavage might be a part of an early apoptotic response, two experiments were designed: 1) visualization of cytochrome C (Cyc1)-GFP fusion localization, and 2) estimation of the percentage of apoptotic cells in cultures treated with drug doses known to induce exclusively ES7c-cleavage.

As mentioned, one of the earliest indicators of apoptosis is the deterioration of mitochondrial membrane integrity. In order to investigate whether or not this process was occurring in our experimental setup, a Cyc1-GFP fusion was cloned and expressed in cells (See Materials and Methods). Cytochrome c is a component of the electron transport chain. As such it is naturally localized within the mitochondrial membrane. Consequently, when the mitochondrial membrane integrity is compromised, cytochrome c is released into the cytosol (reviewed in: Strich, 2015). In theory, expressing cytochrome c-GFP from a plasmid will allow for observation of cytochrome c localization using a fluorescent microscope.

Cyc1 was cloned in frame with GFP (Green Fluorescent Protein), where GFP was N-terminally fused with Cyc1 as described in Roucou et al., 2000 (see Materials and Methods). We cloned *GFP-CYC1* into 2 μc vector under control of strong constitutive promoter ADH1. Generated plasmid and empty vector-control were then transformed in to yeast *WT BY4741* cells. Western blot analysis conducted with anti-GFP antibodies demonstrated that GFP-Cyc1 is successfully expressed in transformed cells (Figure 11B).

To visualize GFP-Cyc1 localization in normal (untreated) and stressed cells, we used live fluorescent microscopy. To visualize mitochondria, we transformed cells with mtRED containing plasmid (courtesy of Dr. Katrina Cooper). The mtRED represents a protein marker for mitochondria and is composed of a RFP (Red Fluorescent Protein) derivative fused with a mitochondrial-targeting sequence. For consistency, treatment conditions were matched to the

experiment conducted earlier (Figure 10A). Cells were either not treated, or treated with 0.2mM H_2O_2. The results are somewhat obfuscated. Although the mitochondria are visible on the red fluorescent channel, the green fluorescent channel reveals blurry, delocalized cytochrome c (Figure 11A). It appears that the Cyc1-GFP was overexpressed from the plasmid, resulting in fluorescent GFP signal that was dispersed throughout the entire cell. Due to time constraints, this particular assay was not resolved and requires significant additional fine-tuning.

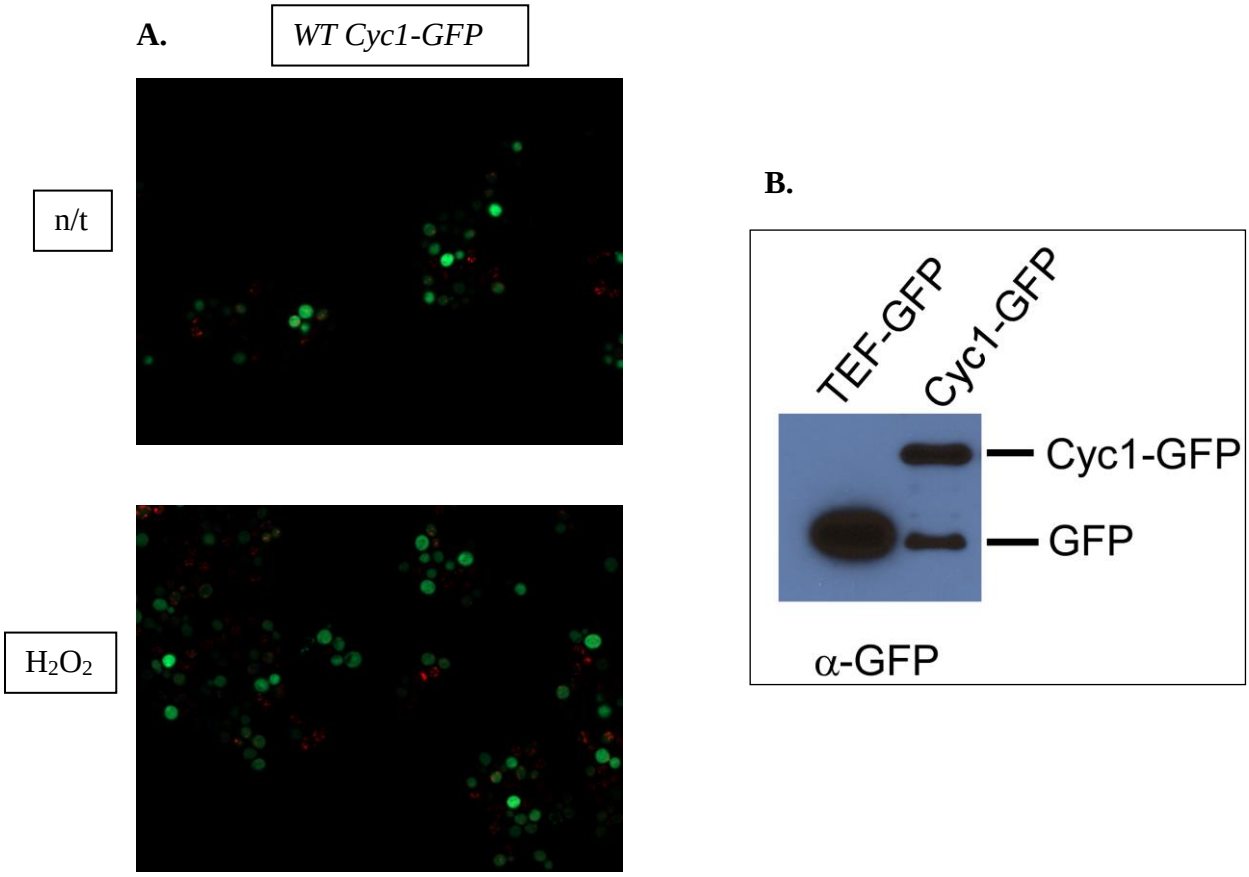

Figure 11. Detection of mitochondrial membrane integrity. A) Cells expressing Cyc1-GFP plasmid were subjected to the same treatment conditions. Expression of mtRED was also visible in these cells allowing for visualization of mitochondria. B) Western blot analysis showing that Cyc1-GFP is expressed as indicated by higher-weight molecular band. Antibody was raised against GFP.

Since the Cyc1-GFP approach failed to provide acceptable results, an additional assay was employed for detecting those cells that just turned on the programmed cell death program. As such, an assay based on detection of translocation of the membrane localized phosphatidylserine – an early apoptotic marker, was considered next (Madeo et al., 1997). Annexin V is a protein that recognizes phosphatidylserine when this phospholipid is exposed on the surface of the cell (i.e. during apoptosis). Conjugating a fluorophore to Annexin V allows for the detection of apoptosis via flow cytometry. This is precisely the instrument that was used to evaluate apoptosis in cells under our established treatment conditions. Samples treated with low-dose menadione and H_2O_2 were processed and analyzed with an Annexin V-FITC assay kit. As a control for Annexin V staining experiment, we included 2 hour-long 2mM H_2O_2 treatment, as these conditions were documented to induce apoptosis (Mroczek and Kufel, 2008). After Annexin V staining, samples were analyzed by flow cytometry. Results were analyzed using FlowJo® analysis software and presented in Figure 12. In each individual readout, the peak on the left is the unstained cell population, while the peak on the right represents the number of cells in the apoptotic population. The number above the apoptotic peak indicates the number of cells in that peak as a percentage of the total cell population. Across all samples, with the exception of 2mM H_2O_2 treatment, the amount of apoptotic cells is less than 8% of the total population. Although treatment with 2mM H_2O_2 produces a much higher number of apoptotic cells, it is important to realize that this concentration and treatment time is much more extreme than the previous experiments. Consequently, cells are most likely dead or in the process of dying. The results of Annexin V staining argues against our hypothesis that ES7c-cleavage represents "an early marker of apoptosis."

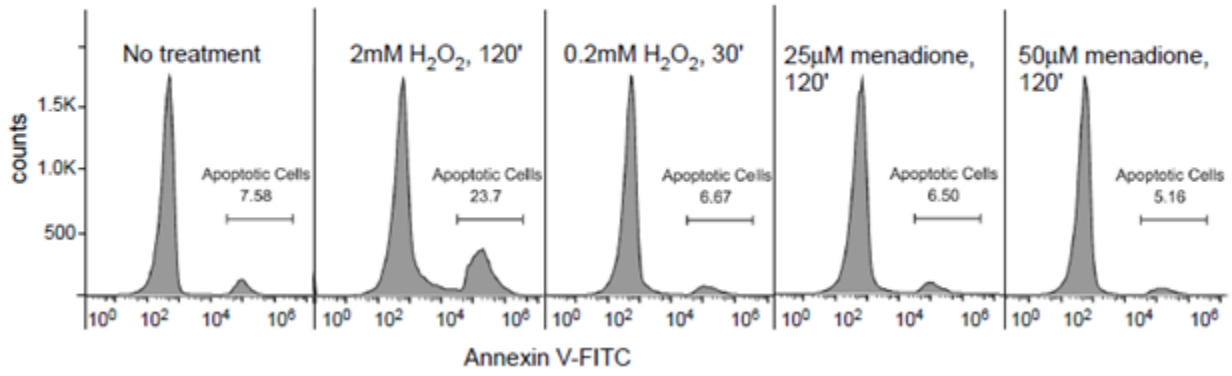

Figure 12. ES7c-cleavage is not a product of apoptosis. *WT* cells were treated identically to cells in panel A. Samples were run through flow cytometer and results were analyzed. Numbers labeled on the curve represents the percentage of cells in apoptosis.

4.4 ES7c-cleavage as the result of targeting from an intracellular source.

The final question of this project was aimed at examining whether intracellular sources of ROS might contribute to the ES7c-cleavage formation. Possibilities for these sources included organelles that have been studied extensively in regard to ROS generation including the ER and the mitochondria (reviewed in: Strich, 2015). The mitochondria was the first choice for experimental inquiry. The idea was to increase release of ROS from the mitochondria and observe if there is a change in the ES7c-fragmentation. To do this, the use of rotenone was employed. Rotenone is an isoflavone capable of inhibiting Complex I of the ETC (Wang et al., 2010). Complex I is an oxidoreductase that transfers two electrons from NADH to ubiquinone. As such, this complex is susceptible to leaking electrons oxygen resulting in the release of ROS.

In this assay, *WT* cells were treated with varying concentrations of rotenone to induce ROS production from the mitochondria. ROS-inducing drugs (menadione) were also added to

the assay so as to provide reference in the form of a positive control. Northern hybridization results show a strong ES7c-cleavage fragment in menadione treatment, but no abundant fragmentation products in rotenone-treated samples (Figure 13A). This lends support to the inference that ES7c-cleavage is not induced by mitochondrial sources of ROS.

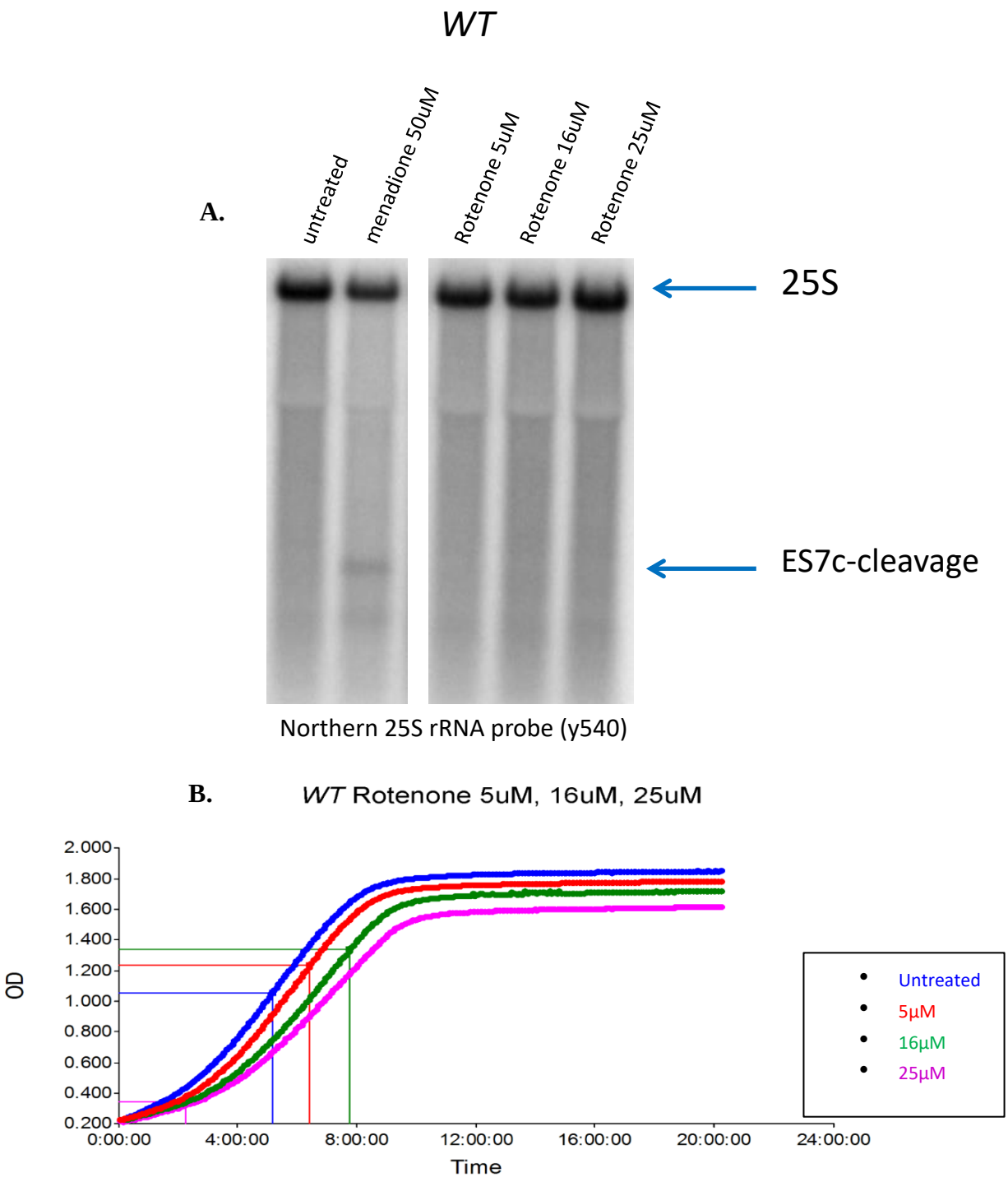

Figure 13. Mitochondrial-sourced ROS. A) Northern hybridization of *WT* cells treated with the Complex I inhibitor, rotenone, as well menadione for comparison. Concentrations are indicated in the figure. B) Growth curves of cells treated with indicated concentrations of rotenone over a period of 24 hours. Note: samples were grown in YPDA media.

Given the results of the previous experiment with rotenone, there was a possibility that cells may have become unviable upon treatment with rotenone. For this reason, growth curves of treated cells were recorded by measuring the OD_{600} over a 24 hour period using a microplate reader. *WT* cells were treated with various concentrations of rotenone, and OD600 was recorded over a 24 hour period. We found no significant differences between untreated and rotenone-treated cells in respect of growth (Figure 13B). One possible explanation may have simply been that the drug was inactive. Nonetheless, the Northern hybridization results (Figure 13A) and growth curve data (Figure 13B) that was collected in our lab suggest that ES7c-cleavage is not a response to mitochondrial ROS.

The second organelle tested for being a potential source of intracellular ROS was the Endoplasmic Reticulum (ER). In order to address this possibility, the ER would need to be stressed to overproducing ROS. Previous data has shown that defective protein folding in the ER can lead to an upregulation of ROS (Tu and Weissman, 2004). Defective protein folding activates the Unfolded Protein Response in the ER. It is known that the antibiotic, tunicamycin, is capable of inducing the UPR in cells (Thomas et al., 2015; Li et al., 2017). Knowing this, an experiment was designed using tunicamycin to induce the UPR in cells and upregulate ROS production from the ER. As with earlier experiments, the *tsa1Δ* was used due to its increased sensitivity to DTT (Figure 3B). In addition, *ire1Δ* cells were also included. In yeast, Ire1 is the kinase responsible for regulating Hac1, ultimately activating the UPR. An important control in this experimental design was the inclusion of a probe to detect Hac1 in both spliced ($HAC1^{i}$) and non-spliced form (HAC1). Spliced form of Hac1 indicates activation of the UPR (Gonzalez et al., 1999). This allows for confirmation regarding whether or not the UPR is activated. Upon activation of the UPR, ES7c-cleavage disappears (Figure 14). As expected, formation of $HAC1^{i}$

was completely blocked in strains carrying the deletion of *ire1* upon ER-stress inducing drug treatments (Figure 14, bottom panel). ES7c-cleavage fragment was still observed in *tsa1Δ ire1Δ* cells upon DTT, but not Tm, treatment (Figure 14, top panel). All together this data indicates cleavage of 25S rRNA in the ES7c region is not a part of the UPR.

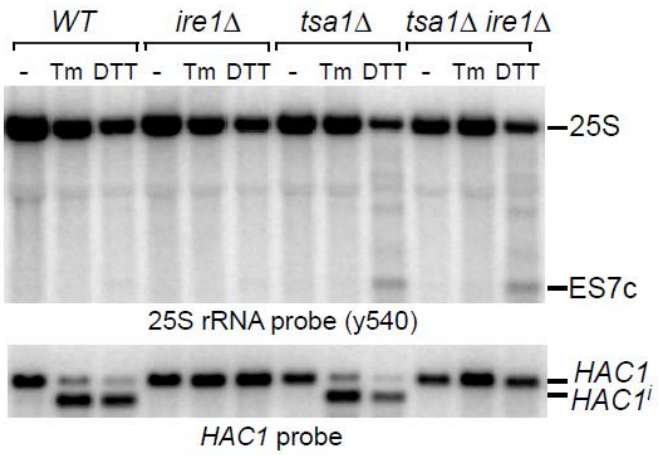

Figure 14. ES7c-cleavage is not part of the UPR. Cultures were grown overnight, diluted to OD_{600}≈0.3, grown for 2 hours at 30°C, and treated with 20mM DTT or 1µg/mL tunicamycin (Tm) for 2 hours. RNA was extracted and probe via Northern hybridization. (Figure courtesy of Natalia Shcherbik).

5. Discussion

This project set out to pursue a new endeavor in the laboratory. The main purpose for this work was to develop the experimental foundation on which to build an investigation into the nature of the endonucleolytic cleavage of 25S rRNA. During preliminary experimentation, a similar fragmentation was revealed to occur upon treatment with DTT (Figure 3A&B). Primer extension allowed this cleavage site to be mapped to the "c" loop region of ES7 region of 25S rRNA (Figure 3C). Using publicly available crystal structures, and the primer extension mapping of this region a digital visualization of our cleavage site was created (Figure 4).

Next we tested different drugs that affect oxidation conditions to determine if ES7c-cleavage is related to redox conditions. *WT* cells were treated with menadione, and plumbagin. Northern hybridization using probes for 25S revealed the presence of ES7c-cleavage fragments (Figure 5). Consequently, this procured the possibility that ES7c-cleavage is a resultant, or a cellular response to an abnormal increase in ROS concentration.

Before deciding to fully invest resources and time into this project, one experiment remained: determining whether ES7c-cleavage was simply a result, or if it was indeed a substantial phenomenon. Addressing this involved the use of time course treatments and post-treatment time courses, as well as titration assays with the various drugs. Treatment time-courses allowed for determination that ES7c-cleavage fragments are formed quickly during treatment with DTT (Figure 6A) and in dose-dependent matter (Figure 6B). Furthermore, treated cells were harvested at time intervals post-treatment and ES7c-cleavage fragmentation was observed. The results of this post-treatment time course show stability of the fragment over time (Figure 6C). Having established that this cleavage product was substantial, further inquiry into the nature of the cleavage was undertaken.

Since this was a phenomenon brand new to the laboratory, there were not yet conceived protocols or procedures to investigate this particular event. Therefore, the first part of this project was heavily focused on founding reliable methods to detect ROS within our experimental parameters. The first ROS-detection assay involved the use of dihydroethidium to visualize changes in levels of superoxides. After much trial and error, conditions were finally identified that produced replicable images of changes in superoxide levels (Figure 7). These assay protocol conditions were further verified using *sod1Δ* and *sod2Δ* strains under the same treatment conditions (Figure 8A). These strains, deficient for superoxide dismutases, will naturally have a higher level of superoxide radicals. Comparing imaging results of the mutants to *WT* (Figure 7 & 8A) we can see that indeed the developed assay is capable of superoxide detection. Moreover, ES7c-cleavage in *sod1Δ* cells treated with ROS-inducers did not show a significant change in amount of fragmentation (Figure 8B & C). In conclusion, this evidence indicates that ES7c-cleavage is unlikely to be the resultant of superoxide influence.

Once a means of detecting superoxide radicals was established, the next focus became establishing a process to measure hydrogen peroxide. After researching various available detectors, Amplex Red detection approach was chosen as the one, which provides the most replicable results (Figure 9A). Moreover, treatment with ROS-inducing drugs resulted in ES7c-cleavage (Figure 9B). Up to this point there was an increasingly supported idea that H_2O_2 was responsible for ES7c-cleavage. In order to solidify this conclusion, the scavenger, ebselen, was used to neutralize H_2O_2. As suspected, ES7c-cleavage diminished significantly when intracellular H_2O_2 levels were reduced with ebselen compared to cells that did not receive ebselen pretreatment (Figure 9C). Taken together, these results imply that hydrogen peroxide is the ROS responsible for ES7c-cleavage.

Cells treated with ROS-inducers consequently experience oxidative stress. Stressed cells retain the option to undergo programmed cell death. The next major part of this project was to determine whether ES7c-cleavage was a product of apoptosis. As mentioned earlier, this type of phenomenon was brand new to our laboratory and as such, we lacked apoptosis-detection protocols to properly investigate our observations within our specific laboratory settings. Three experimental approaches were chosen to determine whether ES7c-cleavage inducing treatments ultimately induce apoptosis as well. The first of these approaches involved the knockout strains, *yca1Δ*, and *aif1Δ*, which were nulls for factors involved in mid-to-late apoptosis. Although this initial experiment indicated ES7c-cleavage was unlikely to be a part of mid-to-late apoptosis (Figure 10A), the question whether it occurs at the initial stage of the programmed cell death program remained open.

Addressing apoptosis further required the exploitation of earlier signs of programmed cell death. The second experimental approach involved a transformed yeast strain expressing cytochrome c-GFP from a plasmid. This approach was designed on the premise that mitochondrial membrane deterioration is one of the earliest events in apoptosis (reviewed in Strich, 2015). Cytochrome c is naturally localized in the mitochondrial membrane. When the membranes are compromised, cytochrome c re-localizes to cytosol. Cyc1-GFP fusion expression vector was generated on 2µc plasmid background (see Materials and Methods) and its expression was tested via Western blot analysis (Figure 11B). Using *WT* cells expressing the transformed cytochrome c-GFP, samples were left untreated or were given 0.2mM H_2O_2 and observed under a fluorescent microscope (Figure 11A). Cells expressing cytochrome c-GFP also expressed mtRED allowing for visualization of the mitochondria. After numerous attempts, results remained less than satisfactory. Cytochrome c-GFP was dispersed throughout the cell,

even in the cells that were not treated with oxidative-stress inducers (Figure 11A). One explanation for the continuous delocalization may be overexpression of exogenous protein. This would cause more cytochrome c-GFP to be expressed than the cell is capable of housing in the mitochondria. Therefore the excess cytochrome c-GFP would remain dispersed throughout the cytoplasm. Alternatively, it is possible that N-terminal GFP addition to Cyc1 might inhibit efficient localization of this fusion protein to the mitochondria. We used the outline published in Roucou et al., 2000, to construct GFP-fusion of Cyc1, therefore we believe that in our case, it might be a combination of high protein expression and inefficient mitochondria targeting what made Cyc1-GFP-based approach unsuccessful.

Acquiring the poor results of the cytochrome c-GFP based approach, we used an alternative approach to measure early apoptotic cell-percentage upon various conditions. Another early hallmark of apoptosis is the translocation of phosphatidylserine to the outer membrane of the cell. This allows for the use of Annexin V, which binds phosphatidylserine. Annexin V conjugated to the fluorophore FITC, allowed for detection of apoptotic cells within our experimental conditions, using flow cytometry. Establishing this protocol was very time consuming. It required the modification of existing protocols, with the addition of steps necessary when working with yeast to create spheroplasts. This spheroplasting aspect of the Annexin V assay requires removal of the yeast cell wall so that Annexin V may bind. Only once the spheroplasting process was ironed out, could the rest of the Annexin V protocol be finalized. After the initial trial-and-error process, a procedure was eventually established that would allow the laboratory to use this technique in the future. With the guidance of this new protocol, *WT* cells were treated with the oxidative stress-inducers H_2O_2, and menadione, exposed to Annexin V-FITC, and analyzed via flow cytometry. Results were quite favorable showing remarkably

low percentages of apoptotic cells under our standard treatment conditions that are able to induce ES7c-cleavage (Figure 12). Results of this Annexin V staining assay support our genetic approach (Figure10A) in concluding that ES7c-cleavage is not an apoptotic event.

So far, protocols have been established and validated to allow our laboratory to future research ROS-dependent phenomena, as well as investigate the programmed cell death. Moreover, evidence has been presented showing that ES7c-cleavage occurs in response to hydrogen peroxide, and the cleavage event is not a part of apoptosis. The final aim of this project was to begin an investigation into possible sources causing the ES7c-cleavage. Possibilities for experimental inquiry included the ER, and the mitochondria.

Investigating the mitochondria as a possible ROS source responsible for the cleavage, the Complex I inhibitor, rotenone, was used. Theoretically, an increase in ES7c-cleavage intensity would indicate that the cleavage may be in response to mitochondrial stress. However, based on the results of this assay, that hypothesis cannot be concluded or disproven. Probing for 25S rRNA, Northern hybridization of drug-treated *WT* cells produced data showing no significant cleavage of ES7c when compared to the menadione-treated positive control (Figure 13A). Based on the Northern hybridization alone, treatment with rotenone had no impact on ES7c-cleavage.

The results prompted further investigation in hopes of revealing the cause of the ineffective treatment. Cells treated with ROS-inducing drugs are obviously put under stress. One possibility to the results was thought to be cell viability. *WT* cells were given rotenone at various concentrations and allowed to grow for 24 hours in YPDA media. OD_{600} readings were taken at set intervals. The resulting growth curves indicate slightly reduced viability as the drug concentrations increase. However, cells retained adequate viability across the range of drug concentrations (Figure 13B). Furthermore, all concentrations used in the previous Northern

hybridization (Figure 13A) allowed for acceptable viability of cells, further providing evidence that the observed effect was real and that rotenone does not affect ES7c-cleavage in that experiment. It must be noted that one possibility for the observed results may have been that our rotenone stock was inactive or poor in quality. Due to the time constraints of the project, exploration into mitochondrial ROS as the potential source of ES7c-cleavage was not further explored.

Another source of intracellular ROS and possible cause of ES7c-cleavage comes from the ER (see Section 4.4). The experimental design for this line of inquiry employed activation of the UPR in the ER, which has been shown to increase levels of ROS from the ER (Haynes et al., 2004). Tunicamycin treatment was the tool of choice to activate the UPR and serve as a control. DTT has also been shown to activate the UPR. In order to monitor the activation status of the UPR, probes capable of detecting non-spliced/inactive Hac1 (HAC1) and spliced/activated Hac1 ($HAC1^{i}$) were exploited. Additionally, *ire1Δ* strains were used that would be incapable of activating the UPR. The strain *tsa1Δ* was also included because this mutant has shown strong ES7c-cleavage effect upon treatment with DTT (Figure 3B). Double deletion-mutant, *tsa1Δ ire1Δ*, was also included in the assay. Samples were left untreated, treated with 20mM DTT, or 1µg/mL tunicamycin. As expected, strains containing the *IRE1* deletion did not display $HAC1^{i}$ (Figure 14, bottom panel). Furthermore, cells treated with tunicamycin failed to exhibit ES7c-cleavage fragments. Strains *tsa1Δ*, and *tsa1Δ ire1Δ* treated with DTT did in fact display ES7c-cleavage product whether $HAC1^{i}$ was present or not (Figure 14, bottom panel). This data show that ES7c-cleavage is not involved in the UPR.

6. Summary and Conclusion

Documentation of 25S rRNA fragment formation in the ES7c region was first made in 2008 (Mroczek and Kufel, 2008). Since then there has been no thorough follow up to the observed phenomenon. Specializing in ribosome and RNA research, this particular published data sparked interest. Various findings have shown that transcriptional factors can be affected when a cell is experiencing stressful conditions. Translation factors that function during initiation (Shenton et al., 2006), elongation (Nagano et al., 2015), and termination (Doronina et al., 2015) may all be affected. After some initial experimentation showing ES7c-cleavage during treatment with the ROS-inducing drugs DTT and H_2O_2 (Figure 3), this project was born.

Never before had our laboratory studied cellular stress, ROS-stress, or apoptosis. Consequently, there were no protocols written or developed for our laboratory resources. As such, the first part of this project was refining techniques that would work under the conditions necessary to study ES7c-cleavage and further ROS, or apoptosis endeavors. Results from this section of the project were able to provide a means of detecting two types of ROS: 1) superoxide radicals (Figures 7 & 8), and 2) hydrogen peroxide (Figure 9).

The next goal was to design a standardized procedure that our laboratory would be able to use to detect apoptosis. The initial choice was to exploit mitochondrial membrane deterioration that occurs during apoptosis. Doing this required cloning a cytochrome c-GFP vector that could be transformed and expressed in *WT* yeast cells. Although the transformation and cloning were both successes, the cytochrome c-GFP failed to localize to the mitochondria (Figure 11A). Despite the setback, the next apoptosis-detection technique involved the Annexin V assay. Once a protocol was established for the procedure, the assay was a success in our

experimental conditions (Figure 12). Moreover, the protocols that were created are capable of being used in future projects.

The final portion of this project investigated possible intracellular sources of ROS that may be responsible for ES7c-cleavage. Based on available literature (see Section 4.4), the ER and the mitochondria were chosen as prime suspects. The results presented for the investigation into mitochondria-sourced ROS indicated that ES7c-cleavage is not affected by mitochondrial ROS (Figure 13). However, time constraints restricted further exploration or alternative approaches to address this experiment. In order to investigate the ER as a source, the ER was stressed to induce the UPR. It can be concluded from this experiment that the UPR is not responsible for ES7c-cleavage (Figure 14). With that being said, the ER itself cannot be ruled out as a source of ROS that causes cleavage.

The major limiting factor of this project was time. There are multiple future directions in which this project can be taken. One idea is to further investigate the mitochondria as the cause of ES7c-cleavage. A genetic approach may be taken to do this, which would utilize *ndi1Δ*, and *coq7Δ* strains and expose them to ROS-inducing conditions used throughout this project. *NDI1* codes for the yeast-equivalent of NADH:ubiquinone oxidoreductase (Marres et al., 1991). Essentially, this gene encodes for Complex I of the ETC in yeast. *COQ7* codes for Coq7, which is responsible for ubiquinone synthesis in yeast (Jonassen et al., 1998). Using these strains may allow further elucidation into the relationship between ROS from the mitochondria and ES7c-cleavage.

The time constraint also restricted full investigation into the ER as the source of ES7c-cleavage. One suggestion for a future experiment is to use an *ero1Δ* mutant. *ERO1* in yeast,

encodes for a thiol oxidase required for oxidative protein folding in the ER (Frand and Kaiser, 1998). Ero1 has also been shown to be capable of producing hydrogen peroxide (Zito, 2015).

Altogether, this project has established procedural techniques for our laboratory to use in the future. Projects to come will be able to rely on the ROS-detection, and programmed cell death protocols that were developed as a part of this project. Furthermore, this project provides a foundation to continue the work on the investigation of ES7c-cleavage. Building upon the groundwork laid in this project will provide the opportunity to elucidate the complete nature of this endonucleolytic cleavage of 25S rRNA. It has been shown that mature tRNA fragments are capable of targeting ribosomes and regulating gene expression (Gebetsberger et al., 2012; Anderson and Ivanov, 2014). If rRNA turns out to be capable of similar stress signaling function, a better understanding of specialized RNA may emerge. The results of such a venture could provide extensive insight into the specifics of transcriptional effects cells experience under common stress conditions, such as ROS, that are associated with ailments ranging from neurodegenerative disease to the aging process.

References

Akerfelt, M., Morimoto, R.I., and Sistonen, L. (2010). Heat shock factors: integrators of cell stress, development and lifespan. Nat. Rev. Mol. Cell Biol. *11*, 545–555.

Anderson, P., and Ivanov, P. (2014). tRNA fragments in human health and disease. FEBS Lett. *588*, 4297–4304.

Antelmann, H., and Helmann, J.D. (2011). Thiol-based redox switches and gene regulation. Antioxid. Redox Signal. *14*, 1049–1063.

Avery, S.V. (2011). Molecular targets of oxidative stress. Biochem. J. *434*, 201–210.

Back, S.H., Schröder, M., Lee, K., Zhang, K., and Kaufman, R.J. (2005). ER stress signaling by regulated splicing: IRE1/HAC1/XBP1. Methods *35*, 395–416.

Bannister, J.V., Bannister, W.H., and Rotilio, G. (1987). Aspects of the structure, function, and applications of superoxide dismutase. CRC Crit. Rev. Biochem. *22*, 111–180

Barros, M.H., Netto, L.E.S., and Kowaltowski, A.J. (2003). H(2)O(2) generation in Saccharomyces cerevisiae respiratory pet mutants: effect of cytochrome c. Free Radic. Biol. Med. *35*, 179–188.

Baxter, C.J., Redestig, H., Schauer, N., Repsilber, D., Patil, K.R., Nielsen, J., Selbig, J., Liu, J., Fernie, A.R., and Sweetlove, L.J. (2007). The metabolic response of heterotrophic Arabidopsis cells to oxidative stress. Plant Physiol. *143*, 312–325.

Ben-Shem, A., Garreau de Loubresse, N., Melnikov, S., Jenner, L., Yusupova, G., and Yusupov, M. (2011). The structure of the eukaryotic ribosome at 3.0 Å resolution. Science *334*, 1524–1529.

Biaglow, J.E., and Kachur, A.V. (1997). The generation of hydroxyl radicals in the reaction of molecular oxygen with polyphosphate complexes of ferrous ion. Radiat. Res. *148*, 181–187.

Carmel-Harel, O., Stearman, R., Gasch, A.P., Botstein, D., Brown, P.O., and Storz, G. (2001). Role of thioredoxin reductase in the Yap1p-dependent response to oxidative stress in Saccharomyces cerevisiae. Mol. Microbiol. *39*, 595–605.

Chae, H.Z., Robison, K., Poole, L.B., Church, G., Storz, G., and Rhee, S.G. (1994a). Cloning and sequencing of thiol-specific antioxidant from mammalian brain: alkyl hydroperoxide reductase and thiol-specific antioxidant define a large family of antioxidant enzymes. Proc. Natl. Acad. Sci. U.S.A. *91*, 7017–7021.

Chae, H.Z., Chung, S.J., and Rhee, S.G. (1994b). Thioredoxin-dependent peroxide reductase from yeast. J. Biol. Chem. *269*, 27670–27678.

Chassé, H., Boulben, S., Costache, V., Cormier, P., and Morales, J. (2017). Analysis of translation using polysome profiling. Nucleic Acids Res. *45*, e15.

Cobine, P.A., Ojeda, L.D., Rigby, K.M., and Winge, D.R. (2004). Yeast contain a non-proteinaceous pool of copper in the mitochondrial matrix. J. Biol. Chem. *279*, 14447–14455.

de la Cruz, J., Karbstein, K., and Woolford, J.L. (2015). Functions of ribosomal proteins in assembly of eukaryotic ribosomes in vivo. Annu. Rev. Biochem. *84*, 93–129.

D'Autréaux, B., and Toledano, M.B. (2007). ROS as signalling molecules: mechanisms that generate specificity in ROS homeostasis. Nat. Rev. Mol. Cell Biol. *8*, 813–824.

D. J. Jamieson, "Oxidative stress responses of the yeast Saccharomyces cerevisiae," Yeast, vol. 14, no. 16, pp. 1511–1527, 1998.

Doronina, V.A., Staniforth, G.L., Speldewinde, S.H., Tuite, M.F., and Grant, C.M. (2015). Oxidative stress conditions increase the frequency of de novo formation of the yeast [PSI+] prion. Mol. Microbiol. *96*, 163–174.

Eisenberg, T., Büttner, S., Kroemer, G., and Madeo, F. (2007). The mitochondrial pathway in yeast apoptosis. Apoptosis *12*, 1011–1023.

Engel, C., Sainsbury, S., Cheung, A.C., Kostrewa, D., and Cramer, P. (2013). RNA polymerase I structure and transcription regulation. Nature *502*, 650–655.

Frand, A.R., and Kaiser, C.A. (1998). The ERO1 gene of yeast is required for oxidation of protein dithiols in the endoplasmic reticulum. Mol. Cell *1*, 161–170.

Gebetsberger, J., Zywicki, M., Künzi, A., and Polacek, N. (2012). tRNA-derived fragments target the ribosome and function as regulatory non-coding RNA in Haloferax volcanii. Archaea *2012*, 260909.

Glossary of class names of organic compounds and reactivity intermediates based on structure (IUPAC Recommendations 1995)). PAC, 1995, *67*, 1307

Gómez Ramos, L.M., Smeekens, J.M., Kovacs, N.A., Bowman, J.C., Wartell, R.M., Wu, R., and Williams, L.D. (2016). Yeast rRNA Expansion Segments: Folding and Function. J. Mol. Biol. *428*, 4048–4059.

Gonzalez, T.N., Sidrauski, C., Dörfler, S., and Walter, P. (1999). Mechanism of non-spliceosomal mRNA splicing in the unfolded protein response pathway. EMBO J. *18*, 3119–3132.

Green, D.R., and Kroemer, G. (2004). The pathophysiology of mitochondrial cell death. Science *305*, 626–629.

Haynes, C.M., Titus, E.A., and Cooper, A.A. (2004). Degradation of misfolded proteins prevents ER-derived oxidative stress and cell death. Mol. Cell *15*, 767–776.

Held, K.D., Sylvester, F.C., Hopcia, K.L., and Biaglow, J.E. (1996). Role of Fenton chemistry in thiol-induced toxicity and apoptosis. Radiat. Res. *145*, 542–553.

Imlay, J.A. (2008). Cellular defenses against superoxide and hydrogen peroxide. Annu. Rev. Biochem. *77*, 755–776.

Izawa, S., Maeda, K., Sugiyama, K., Mano, J., Inoue, Y., and Kimura, A. (1999). Thioredoxin deficiency causes the constitutive activation of Yap1, an AP-1-like transcription factor in Saccharomyces cerevisiae. J. Biol. Chem. *274*, 28459–28465.

Jang, H.H., Lee, K.O., Chi, Y.H., Jung, B.G., Park, S.K., Park, J.H., Lee, J.R., Lee, S.S., Moon, J.C., Yun, J.W., et al. (2004). Two enzymes in one; two yeast peroxiredoxins display oxidative stress-dependent switching from a peroxidase to a molecular chaperone function. Cell *117*, 625–635.

Jonassen, T., Proft, M., Randez-Gil, F., Schultz, J.R., Marbois, B.N., Entian, K.D., and Clarke, C.F. (1998). Yeast Clk-1 homologue (Coq7/Cat5) is a mitochondrial protein in coenzyme Q synthesis. J. Biol. Chem. *273*, 3351–3357.

Kaya, A., Gerashchenko, M.V., Seim, I., Labarre, J., Toledano, M.B., and Gladyshev, V.N. (2015). Adaptive aneuploidy protects against thiol peroxidase deficiency by increasing respiration via key mitochondrial proteins. Proc. Natl. Acad. Sci. U.S.A. *112*, 10685–10690.

Kent, T., Lapik, Y.R., and Pestov, D.G. (2009). The 5' external transcribed spacer in mouse ribosomal RNA contains two cleavage sites. RNA *15*, 14–20.

Klaunig, J.E., and Kamendulis, L.M. (2004). T HE R OLE OF O XIDATIVE S TRESS IN C ARCINOGENESIS. Annual Review of Pharmacology and Toxicology *44*, 239–267.

Kuge, S., Jones, N., and Nomoto, A. (1997). Regulation of yAP-1 nuclear localization in response to oxidative stress. EMBO J. *16*, 1710–1720.

Lee, J.-W., and Helmann, J.D. (2006). The PerR transcription factor senses H2O2 by metal-catalysed histidine oxidation. Nature *440*, 363–367.

Lee, J.Y., Jun, D.Y., Park, J.E., Kwon, G.H., Kim, J.-S., and Kim, Y.H. (2017). Pro-Apoptotic Role of the Human YPEL5 Gene Identified by Functional Complementation of a Yeast moh1Δ Mutation. J. Microbiol. Biotechnol. *27*, 633–643.

Li, Q., Wei, H., Liu, L., Yang, X., Zhang, X., and Xie, Q. (2017). Unfolded protein response activation compensates ER-associated degradation deficiency in Arabidopsis. J Integr Plant Biol.

Lim, J.C., Choi, H.-I., Park, Y.S., Nam, H.W., Woo, H.A., Kwon, K.-S., Kim, Y.S., Rhee, S.G., Kim, K., and Chae, H.Z. (2008). Irreversible oxidation of the active-site cysteine of peroxiredoxin to cysteine sulfonic acid for enhanced molecular chaperone activity. J. Biol. Chem. *283*, 28873–28880.

Ling, J., and Söll, D. (2010). Severe oxidative stress induces protein mistranslation through impairment of an aminoacyl-tRNA synthetase editing site. Proc. Natl. Acad. Sci. U.S.A. *107*, 4028–4033.

Longtine, M.S., McKenzie, A., Demarini, D.J., Shah, N.G., Wach, A., Brachat, A., Philippsen, P., and Pringle, J.R. (1998). Additional modules for versatile and economical PCR-based gene deletion and modification in Saccharomyces cerevisiae. Yeast *14*, 953–961.

Madeo, F., Fröhlich, E., and Fröhlich, K.U. (1997). A yeast mutant showing diagnostic markers of early and late apoptosis. J. Cell Biol. *139*, 729–734.

Madeo, F., Herker, E., Maldener, C., Wissing, S., Lächelt, S., Herlan, M., Fehr, M., Lauber, K., Sigrist, S.J., Wesselborg, S., et al. (2002). A caspase-related protease regulates apoptosis in yeast. Mol. Cell *9*, 911–917.

Mansour, F.H., and Pestov, D.G. (2013). Separation of long RNA by agarose-formaldehyde gel electrophoresis. Anal. Biochem. *441*, 18–20.

Marinho, H.S., Real, C., Cyrne, L., Soares, H., and Antunes, F. (2014). Hydrogen peroxide sensing, signaling and regulation of transcription factors. Redox Biol *2*, 535–562.

Marres, C.A., de Vries, S., and Grivell, L.A. (1991). Isolation and inactivation of the nuclear gene encoding the rotenone-insensitive internal NADH: ubiquinone oxidoreductase of mitochondria from Saccharomyces cerevisiae. Eur. J. Biochem. *195*, 857–862.

Mroczek, S., and Kufel, J. (2008). Apoptotic signals induce specific degradation of ribosomal RNA in yeast. Nucleic Acids Res. *36*, 2874–2888.

Nagano, T., Yutthanasirikul, R., Hihara, Y., Hisabori, T., Kanamori, T., Takeuchi, N., Ueda, T., and Nishiyama, Y. (2015). Oxidation of translation factor EF-G transiently retards the translational elongation cycle in Escherichia coli. J. Biochem. *158*, 165–172.

Netzer, N., Goodenbour, J.M., David, A., Dittmar, K.A., Jones, R.B., Schneider, J.R., Boone, D., Eves, E.M., Rosner, M.R., Gibbs, J.S., et al. (2009). Innate immune and chemically triggered oxidative stress modifies translational fidelity. Nature *462*, 522–526.

Nunomura, A., Perry, G., Pappolla, M.A., Wade, R., Hirai, K., Chiba, S., and Smith, M.A. (1999). RNA oxidation is a prominent feature of vulnerable neurons in Alzheimer's disease. J. Neurosci. *19*, 1959–1964.

Nunomura, A., Chiba, S., Kosaka, K., Takeda, A., Castellani, R.J., Smith, M.A., and Perry, G. (2002). Neuronal RNA oxidation is a prominent feature of dementia with Lewy bodies. Neuroreport *13*, 2035–2039.

Ohdate, T., Izawa, S., Kita, K., and Inoue, Y. (2010). Regulatory mechanism for expression of GPX1 in response to glucose starvation and Ca in Saccharomyces cerevisiae: involvement of Snf1 and Ras/cAMP pathway in Ca signaling. Genes Cells *15*, 59–75.

Okazaki, S., Tachibana, T., Naganuma, A., Mano, N., and Kuge, S. (2007). Multistep disulfide bond formation in Yap1 is required for sensing and transduction of H2O2 stress signal. Mol. Cell *27*, 675–688.

Palade, G.E. (1955). A small particulate component of the cytoplasm. J Biophys Biochem Cytol *1*, 59–68.

Pathak, B.K., Mondal, S., and Barat, C. (2017). Inhibition of Escherichia coli ribosome subunit dissociation by chloramphenicol and Blasticidin: a new mode of action of the antibiotics. Lett. Appl. Microbiol. *64*, 79–85.

Pestov, D.G., Lapik, Y.R., and Lau, L.F. (2008). Assays for ribosomal RNA processing and ribosome assembly. Curr Protoc Cell Biol *Chapter 22*, Unit 22.11.

Raina, M., and Ibba, M. (2014). tRNAs as regulators of biological processes. Front Genet *5*, 171.

Rakauskaite, R., and Dinman, J.D. (2008). rRNA mutants in the yeast peptidyltransferase center reveal allosteric information networks and mechanisms of drug resistance. Nucleic Acids Res. *36*, 1497–1507.

Rand, J.D., and Grant, C.M. (2006). The thioredoxin system protects ribosomes against stress-induced aggregation. Mol. Biol. Cell *17*, 387–401.

Rhee, S.G., and Woo, H.A. (2011). Multiple functions of peroxiredoxins: peroxidases, sensors and regulators of the intracellular messenger H_2O_2, and protein chaperones. Antioxid. Redox Signal. *15*, 781–794.

Roucou, X., Prescott, M., Devenish, R.J., and Nagley, P. (2000). A cytochrome c-GFP fusion is not released from mitochondria into the cytoplasm upon expression of Bax in yeast cells. FEBS Lett. *471*, 235–239.

Satheeshkumar, K., and Mugesh, G. (2011). Synthesis and antioxidant activity of peptide-based ebselen analogues. Chemistry *17*, 4849–4857.

Setiey, A., Challamel, M.J., Champsaur, G., Samuel, D., and Courjon, J. (1975). Proceedings: The effects of profound hypothermia with circulatory arrest on the EEG obtained during operation in the newborn. Electroencephalogr Clin Neurophysiol *39*, 555–556.

Shenton, D., Smirnova, J.B., Selley, J.N., Carroll, K., Hubbard, S.J., Pavitt, G.D., Ashe, M.P., and Grant, C.M. (2006). Global translational responses to oxidative stress impact upon multiple levels of protein synthesis. J. Biol. Chem. *281*, 29011–29021.

Sideri, T.C., Koloteva-Levine, N., Tuite, M.F., and Grant, C.M. (2011). Methionine oxidation of Sup35 protein induces formation of the [PSI+] prion in a yeast peroxiredoxin mutant. J. Biol. Chem. *286*, 38924–38931.

Simms, C.L., Hudson, B.H., Mosior, J.W., Rangwala, A.S., and Zaher, H.S. (2014). An active role for the ribosome in determining the fate of oxidized mRNA. Cell Rep *9*, 1256–1264.

Steitz, T.A. (2008). A structural understanding of the dynamic ribosome machine. Nat. Rev. Mol. Cell Biol. *9*, 242–253.

Strich, R. (2015). Programmed Cell Death Initiation and Execution in Budding Yeast. Genetics *200*, 1003–1014.

Suzuki, H., Sakabe, T., Hirose, Y., and Eki, T. (2017). Development and evaluation of yeast-based GFP and luciferase reporter assays for chemical-induced genotoxicity and oxidative damage. Appl. Microbiol. Biotechnol. *101*, 659–671.

Switala, J., and Loewen, P.C. (2002). Diversity of properties among catalases. Arch. Biochem. Biophys. *401*, 145–154.

Tanaka, M., Chock, P.B., and Stadtman, E.R. (2007). Oxidized messenger RNA induces translation errors. Proc. Natl. Acad. Sci. U.S.A. *104*, 66–71.

Thomas, E., Sircaik, S., Roman, E., Brunel, J.-M., Johri, A.K., Pla, J., and Panwar, S.L. (2015). The activity of RTA2, a downstream effector of the calcineurin pathway, is required during tunicamycin-induced ER stress response in Candida albicans. FEMS Yeast Res. *15*.

Thompson, D.M., Lu, C., Green, P.J., and Parker, R. (2008). tRNA cleavage is a conserved response to oxidative stress in eukaryotes. RNA *14*, 2095–2103.

Trotter, E.W., and Grant, C.M. (2002). Thioredoxins are required for protection against a reductive stress in the yeast Saccharomyces cerevisiae. Mol. Microbiol. *46*, 869–878.

Tu, B.P., and Weissman, J.S. (2004). Oxidative protein folding in eukaryotes: mechanisms and consequences. J. Cell Biol. *164*, 341–346.

Wang, N., Miller, C.J., Wang, P., and Waite, T.D. (2017). Quantitative determination of trace hydrogen peroxide in the presence of sulfide using the Amplex Red/horseradish peroxidase assay. Anal. Chim. Acta *963*, 61–67.

Wang, Y., Gulis, G., Buckner, S., Johnson, P.C., Sullivan, D., Busenlehner, L., and Marcus, S. (2010). The MAP kinase Pmk1 and protein kinase A are required for rotenone resistance in the fission yeast, Schizosaccharomyces pombe. Biochem. Biophys. Res. Commun. *399*, 123–128.

Wang, Y., Hao, C., Fu, B., Liu, W., Zhou, X., Zeng, T., Guo, J., and Wang, G. (2015). A novel method to identify and isolate proliferative inflammatory atrophy (PIA) clusters and to extract high-quality PIA RNA. Int J Clin Exp Pathol *8*, 3987–3993.

Winterbourn, C.C., and Hampton, M.B. (2008). Thiol chemistry and specificity in redox signaling. Free Radic. Biol. Med. *45*, 549–561.

Wissing, S., Ludovico, P., Herker, E., Büttner, S., Engelhardt, S.M., Decker, T., Link, A., Proksch, A., Rodrigues, F., Corte-Real, M., et al. (2004). An AIF orthologue regulates apoptosis in yeast. J. Cell Biol. *166*, 969–974.

Wu, C.-Y., Bird, A.J., Winge, D.R., and Eide, D.J. (2007). Regulation of the yeast TSA1 peroxiredoxin by ZAP1 is an adaptive response to the oxidative stress of zinc deficiency. J. Biol. Chem. *282*, 2184–2195.

Xiang, X.-Y., Yang, X.-C., Su, J., Kang, J.-S., Wu, Y., Xue, Y.-N., Dong, Y.-T., and Sun, L.-K. (2016). Inhibition of autophagic flux by ROS promotes apoptosis during DTT-induced ER/oxidative stress in HeLa cells. Oncol. Rep. *35*, 3471–3479.

Yamamoto, A., Ueda, J., Yamamoto, N., Hashikawa, N., and Sakurai, H. (2007). Role of heat shock transcription factor in Saccharomyces cerevisiae oxidative stress response. Eukaryotic Cell *6*, 1373–1379.

Zhang, J., Perry, G., Smith, M.A., Robertson, D., Olson, S.J., Graham, D.G., and Montine, T.J. (1999). Parkinson's disease is associated with oxidative damage to cytoplasmic DNA and RNA in substantia nigra neurons. Am. J. Pathol. *154*, 1423–1429.

Zito, E. (2015). ERO1: A protein disulfide oxidase and H2O2 producer. Free Radic. Biol. Med. *83*, 299–304.

Abbreviations

ATP – adenosine triphosphate

ETC – electron transport chain

UPR – unfolded protein response

ROS – reactive oxygen species

eIF – eukaryotic initiation factor

eRF – eukaryotic release factor

DTT – dithiothreitol

DHE – dihydroethidium

rRNA – ribosomal ribonucleic acid

tRNA – transfer ribonucleic acid

spheroplast – a yeast cell that has had its outer cell wall removed (typically via enzymatic digestion)

Attributions

Figure 1 – created by Ethan Gardner

Figure 2 – created by Ethan Gardner

Figure 3 – work done by Natalia Shcherbik, Ph.D.

Figure 4 – created by Ethan Gardner

Figure 5 – work performed by Dan Shedlovski

Figure 6 – work performed by Ethan Gardner, Natalia Shcherbik, Ph.D., Dan Shedlovksi

Figure 7 – work performed by Ethan Gardner

Figure 8 – work performed by Ethan Gardner, and Natalia Shcherbik, Ph.D.

Figure 9 – work performed by Natalia Shcherbik, Ph.D., and Dan Shedlovksi

Figure 10 – work performed by Ethan Gardner, and Natalia Shcherbik, Ph.D.

Figure 11 – work performed by Ethan Gardner

Figure 12 – work performed by Ethan Gardner and Dan Shedlovski

Figure 13 – work performed by Ethan Gardner

Figure 14 – work performed by Natalia Shcherbik, Ph.D.